University of Alberta

Mechanical Means of Plastic Land Mine Detection

by

David Stephen Skaley ©

A thesis submitted to the Faculty of Graduate Studies and Research in partial fulfillment of the requirements for the degree of Master of Science.

Department of Mechanical Engineering

Edmonton, Alberta

Spring 2001

National Library of Canada
Acquisitions and Bibliographic Services
395 Wellington Street
Ottawa ON K1A 0N4
Canada

Bibliothèque nationale du Canada
Acquisitions et services bibliographiques
395, rue Wellington
Ottawa ON K1A 0N4
Canada

Your file Votre référence

Our file Notre référence

The author has granted a non-exclusive licence allowing the National Library of Canada to reproduce, loan, distribute or sell copies of this thesis in microform, paper or electronic formats.

L'auteur a accordé une licence non exclusive permettant à la Bibliothèque nationale du Canada de reproduire, prêter, distribuer ou vendre des copies de cette thèse sous la forme de microfiche/film, de reproduction sur papier ou sur format électronique.

The author retains ownership of the copyright in this thesis. Neither the thesis nor substantial extracts from it may be printed or otherwise reproduced without the author's permission.

L'auteur conserve la propriété du droit d'auteur qui protège cette thèse. Ni la thèse ni des extraits substantiels de celle-ci ne doivent être imprimés ou autrement reproduits sans son autorisation.

0-612-60499-3

Canada

University of Alberta

Library Release Form

Name of Author: David Stephen Skaley

Title of Thesis: Mechanical Means of Plastic Land Mine Detection

Degree: Master of Science

Year this Degree Granted: 2001

Permission is hereby granted to the University of Alberta to reproduce single copies of this thesis and to lend or sell such copies for private, scholarly, or scientific research purposes only.

The author reserves all other publication and other rights in association with the copyright in the thesis, and except as hereinbefore provided, neither the thesis nor any substantial portion thereof may be printed or otherwise reproduced in any material form whatever without the author's prior written permission.

David Skaley

David Stephen Skaley
#389 Village Drive,
Sherwood Park, Alberta,
Canada. T8A 4W1

Date January 29, 2001

University of Alberta

Faculty of Graduate Studies and Research

The undersigned certify that they have read, and recommend to the Faculty of Graduate Studies and Research for acceptance, a thesis entitled Mechanical Means of Plastic Land Mine Detection submitted by David Stephen Skaley in partial fulfillment of the requirements for the degree of Master of Science.

Dr. K. R. Fyfe (Supervisor)

Dr. R. Brachman

Dr. G. Faulkner

Date JAN 29, 2001

ABSTRACT

Low-cost plastic land mines inflict hardship on civilians in war-torn lands for decades after a conflict is over. Current mine-clearing technologies are either too expensive or too slow and unreliable to find their way into wide-spread use.

The following discussion describes an automated mechanical method for land mine detection motivated by the hand prodder. The purpose of this method is to remove the danger from hand prodding while retaining the ability to determine the identity of hidden objects. To achieve this end, the vibration in a mechanized prodder, produced by contacting a hidden object, is recorded by a computer using an accelerometer mounted on the end of the prodder. The vibration information is broken down into several features which are indicative of the type of object struck. The objects are classified using pattern recognition Adaptive Logic Network (ALN) software which is a form of artificial neural network (ANN) software. The entire process is intended to be automated, thus significantly reducing the risk to field personnel.

ACKNOWLEDGEMENTS

It would not have been possible to write this thesis without the constant support of my loving wife Robyn. She has helped me realize what is most important in my life. For this I am eternally grateful.

I would like to thank my supervisor, Dr. Ken Fyfe, for his patience and support through the writing of this thesis. This was an enjoyable experience due to his good-natured humour and spirit.

CONTENTS

1 Introduction 1

1.1 Detection Technologies 2

1.1.1 Electromagnetic (EM) Induction Metal Detector 3

1.1.2 Ground Penetrating Radar (GPR) 4

1.1.3 Infrared (IR) or Thermal Imaging (TI) 5

1.1.4 Optical Imaging 5

1.1.5 Photon (X-Ray) Backscatter 5

1.1.6 Acoustic and Seismic 6

1.1.7 Nuclear Magnetic Resonance (NMR), Nuclear Quadropole Resonance (NQR), Thermal Neutron Activation (TNA), Neutron Moderation 6

1.1.8 Biosensors, Trace Explosive Detection (TED) 7

1.1.9 Mechanical Detection Methods 7

1.1.10 Hand Held Prodding 7

1.1.11 Heated Probe Tip Prodders 8

1.2 Summary and Motivation of Current Work 8

2 Modeling of Object Prodder Impact System 10

2.1 Single Degree of Freedom Model 11

2.1.1 SDOF Model Assumptions 11

2.1.2 Time Domain Analysis and Features 14

2.1.3 Frequency Domain Analysis and Features 15
2.1.4 SDOF Results 18
2.2 2DOF System, Compressible Soil 22
2.3 Conclusions of Modeling 27

3 Test Equipment and Procedures **28**
3.1 Data Acquisition Hardware and Software 28
3.2 Apparatus and Procedure 29
3.2.1 Apparatus 30
3.2.2 Striking Method 30
3.2.3 Test Objects 32

4 Data Processing and Feature Extraction **34**
4.1 Raw data 34
4.1.1 Initial Noise Removal 35
4.1.2 Averaging a Series of Prodder Strikes 35
4.2 Signal Feature Extraction 39
4.2.1 Time Domain Features 39
4.2.2 Frequency Domain Features 39
4.3 Example of Feature Values 40
4.3.1 Feature Extraction Results 42
4.4 Summary of Feature Extraction 43

5 Artificial Neural Networks and Pattern Recognition **46**
5.1 Feed-Forward Networks with Supervised Learning 46
5.1.1 An Illustrative Example of Object Classification Using Input Features 47
5.2 Adaptive Logic Network (ALN) 50
5.2.1 The ALN Function 50
5.2.2 ALN Learning 51

5.3 ALN Training 53
5.3.1 Object Classification Using an ALN Network 53
5.4 Network Optimization 54
5.4.1 Number of Strikes With Prodder 54
5.4.2 Overtraining the Network 55
5.4.3 Object Numbering and Order 56
5.4.4 Features Attempted and Rejected 57
5.5 ALN Results 57
5.5.1 Results of the Best ALN Classification 58
5.6 Conclusions of ALN Object Classification 59
6 Conclusions and Future Work **62**
6.1 Conclusions of Current Work 62
6.2 Future Research 64
References **66**
A Object Properties **68**
B Theoretical Models for the Prodder and Object Impulse System **70**
B.1 Two Degree of Freedom Model Eigenvalues 70
B.2 Continuous System 72
C Software Programs Used to Identify Object Features **74**
C.1 Averaging the Acceleration Signals 74
C.2 Determination and Storage of Time and Frequency Domain Features . . 76
D Averaged Acceleration Plots for Each Object **78**
E Feature Values for Each Object **83**

List of Figures

2.1 Schematic of the prodder and object system model 12

2.2 Single degree of freedom (SDOF) model of the prodder striking a compressible object 13

2.3 A single degree of freedom model vibration pattern. Only the first half cycle of the response is shown. This mimics the behavior of the prodder bouncing off the object after contact. Also shown are the time domain features of t_{wid} (the width of the pulse) and A (amplitude of the pulse). 16

2.4 The time domain vibration response of a single degree of freedom model with damping using ζ values of 0.2 and 1.5. 17

2.5 The frequency domain response of signals with damping ζ values of 0.2 and 1.5. 19

2.6 2DOF model of the prodder and object impulse system. 23

2.7 The acceleration data from a VS-50 AP mine and a 2DOF model acceleration response. 26

3.1 Schematic drawing of the apparatus use during testing. 31

3.2 Prodder firing mechanism with hook that lifts prodder. 33

4.1 Output from the accelerometer as the prodder strikes the VS-50 AP mine 36

4.2 Processed time signal output from accelerometer as the prodder strikes the VS-50 AP mine 37

4.3 Averaged time signal output from the accelerometer as the prodder strikes the VS-50 AP mine using 10 strikes in succession on a specific region of the mine. 38
4.4 Frequency domain features of the averaged time signal of the VS-50 AP mine. 41
4.5 Scatter plot of the time domain feature t_{wid} and the object classification. 44
4.6 Scatter plot of the standard deviation $\sigma_{t_{wid}}$ of the time domain feature t_{wid} and the object classification. 45

5.1 ALN Classification using the variable t_{wid}. Several lines are used to approximate curvature of a function. The more lines that are used, the better the approximation 52
5.2 A scatter plot of an overtrained ALN output using training data as the input. 60
5.3 A scatter plot of an overtrained ALN output using test data as the input. 60
5.4 ALN output vs. actual class using the test database to evaluate the ALN. 61

D.1 Time domain averaged plot of AP mine VS-50. 79
D.2 Time domain averaged plot of AP mine VS-50 side. 79
D.3 Time domain averaged plot of AP mine PMA-1A. 80
D.4 Time domain averaged plot of AT mine TMA-1. 80
D.5 Time domain averaged plot of AT mine TMA-5A. 81
D.6 Time domain averaged plot of AT mine TMA-4. 81
D.7 Time domain averaged plot of wood object. 82
D.8 Time domain averaged plot of steel object. 82

LIST OF TABLES

2.1 SDOF features using VS-50 AP mine stiffness 21

2.2 SDOF features after normalizing the time domain signals 23

2.3 2DOF model normalized features 28

4.1 Features extracted from 10 averaged VS-50 AP mine signals 44

5.1 Example of features used to train an ANN 51

5.2 Example of an ideal ALN network Output 56

5.3 An overtrained network response to training set data 58

5.4 An overtrained network response to the test data set 58

5.5 Results of the best ALN network evaluated using four of the test sets . . 60

A.1 Physical properties of the objects used during testing 68

D.1 VS-50 AP mine trigger object features 84

D.2 VS-50 AP mine side object features 85

D.3 PMA-1A AP mine object features 86

D.4 TMA-1 AT mine object features 87

D.5 TMA-5A AT mine object features 88

D.6 TMA-4 AT mine object features 89

D.7 Wood object features 90

D.8 Steel object features 91

CHAPTER 1

INTRODUCTION

Land mines are tactical weapons of war designed to explode when their triggering mechanism is set off. The most common trigger type is the pressure exerted when a person or a vehicle passes over the surface of the mine. Typically, an anti-personnel mine (AP mine) is designed to explode when forces greater than 30 to 100N force are placed over its surface. Anti-tank mines (AT mines) will explode when over 900N of force is placed on them.

It is estimated that there are 85 million uncleared landmines scattered in 56 countries around the world.[Hidden Killers, 33] This is only an estimate, however. Because of poorly kept records (and in some cases, no records at all), it is impossible to provide an exact number. In fact, the majority of nations with a landmine problem cannot determine the amount or location of landmines within their borders.[Hidden Killers, 3] Over two million new mines are laid each year while fewer than one hundred thousand are recovered. Thousands of people are maimed or killed each month as a result.

In 1998, Canada initiated a moratorium on land mines, signed by most of the world's countries with the notable exceptions being Russia, China and the U.S. This treaty calls for a complete ban on the production an use of AP land mines. Certainly this treaty is a major step forward in ending the proliferation of AP mine devices. However, it may be said that even if land mine deployment where to stop today,

current methods would require hundreds of years and billions of dollars to eliminate the mines already in place. The cost of mine removal is estimated to be $1000 per mine, and this does not include the additional fiscal demands on infrastructure and health care.[Hidden Killers, 8] The cost of manufacturing a plastic type landmine can be as low as $3 for an AP mine and $75 for an AT mine[Hidden Killers, 2]

Landmines are produced in a vast variety of shapes and sizes. Their construction ranges from hand-made wooden mines to mass-produced plastic mines. Land mines are commonly cylindrically shaped. The type of explosives contained in mines vary and include TNT, RDX, EGDN and, PETN. The amount of explosives range from tens of grams to a few kilograms.[McFee, 2]

The majority of landmines currently made may be defined as low metal content mines. These are predominantly of nonmetallic (usually plastic) construction, having at least one small metallic part such as a firing pin, spring or ball bearing.[McFee, 2]

Most new technologies are developed by the military. The primary objective of the military is in breaching, which is the clearance of a path through a minefield to transport vehicles and troops. Other mines are typically left to humanitarian demining efforts (which do not have the resources of the military) for removal and mine disposal. Several of these methods are described in the following section. This is not intended to be a definitive list, but rather a description of several of the more widely used and technologically promising devices.

1.1 Detection Technologies

Demining, defined as the complete removal of all landmines from an area in order to safeguard civilian populations, aims at 100% accuracy in mine removal. It is recognized that even a few uncleared landmines have potential to cause casualties over time.[Hidden Killers, 16] The first stage in demining is the detection of landmines. Detection schemes concentrate on identifying the difference between the mine and the surrounding soil. Typical high-tech electronic systems include ground penetrating

radar (GPR), infra-red (IR) sensors, and magnetic resonance imaging techniques. Other methods range from biological detection schemes (dog sniffers and insects or bacteria) to simple brute force detonation methods (flails, rollers and plows) and the use of hand-held prodders. These will be discussed in some detail in the following section.

With the exception of the hand prodder, these methods of detecting land mines are not 100% effective. Manual demining at present is considered the most common and reliable means of land clearance. It will probably remain the basic framework for future mine clearance operations.[Focsaneanu, S4.4] Typically, the high-tech solutions do not have the accuracy needed to completely remove landmines. Furthermore, brute force methods can be slow, and frequently destroy road systems as they work. Plows and flails are designed by the military for the purpose of breaching a mine field to allow the passage of military vehicles.

The following technologies are currently either in use or are being actively investigated as possible new methods of detecting land mines. This is not meant to be an exclusive list; only those technologies most likely to produce a workable device were examined. Many of the sensors developed could be used in unison with other sensors to provide better detection when combined. This union is known as data fusion, and appears to be the best solution for detecting both metal and non-metallic mines.

1.1.1 Electromagnetic (EM) Induction Metal Detector

Electromagnetic induction metal detectors were used extensively to detect land mines during the years following World War II. Most land mines were made of ferrous metal, making them relatively easy to detect from the background environment. In order for this method to work, the target object must contain some amount of metal. The EM detector's sensitivity can be increased to detect the low metal content in some plastic mines. However, the increased sensitivity creates many false alarms due to other conductive debris. Even soils with a rich iron content can cause a sensitive

device to indicate a false alarm.

Metal detectors work on the eddy current principle. A weak, high frequency electro-magnetic field is produced. This field is disturbed proportionally to the amount of metal within the field. Typically, metal detectors consist of one or more electric coils made to oscillate at a certain frequency. Changes to the oscillation amplitude give information regarding the metal objects detected. These disturbances are electronically evaluated and the result is made visible by an indication meter and/or an audible tone.

Another similar method is the electromagnetic pulse method. Electromagnetic pulses are emitted and a receiving coil measures how quickly the short-lived magnetic field decays. Metal within the pulse field slows down the rate of decay. Differences in the rate of decay are evaluated and indicated to the operator.[McFee, 21. Craib, 14-15]

1.1.2 Ground Penetrating Radar (GPR)

Currently a great deal of research is underway in which radar or low frequency electromagnetic waves are used to find hidden land mines. Ground penetrating radar (GPR) involves sending an impulse of electromagnetic energy into the ground and recording the amount of backscatter from a buried object. The backscatter signal is compared with that of the surrounding environment. A metal object tends to scatter more than the surroundings while a plastic object would scatter less. One problem with this method is that the signal from plastic mines is obscured somewhat by background noise, thus causing frequent false alarms. Reflections of the radar energy off the surface of the ground can also obscure some land mines. Another major difficulty in the use of GPR is the large amounts of data processing required to successfully identify a land mine target. Research in this area has been the focus of many organizations including the US army.[McFee, 21-22. Craib, 19-20]

1.1.3 Infrared (IR) or Thermal Imaging (TI)

This method utilizes low frequency infrared light that is naturally given off by all hot objects. The thermal characteristics of land mines are different than that of their surroundings. The planting of land mines into the soil causes the flow of heat through the soil to change. By observing the contrast in thermal images using infrared cameras, land mines may thus be detected. However, these contrasts are not as distinct as one would hope. The amount of time that the mine has been in the ground and the depth of burial are factors which must be investigated. Research is currently ongoing into target recognition software which will enhance the detection abilities of this method.[McFee, 23. Craib, 16-18]

1.1.4 Optical Imaging

Visual Spectrum: Using a video camera, target objects are located and classification occurs. Characteristics such as polarization of reflected light and the amount of vegetation growth in an area are recorded. This method is useful only for objects on the surface of the ground and relies heavily on the training of the observer in detecting land mines. By itself, this method has too high a false alarm rate to be justified, but it may prove useful in conjunction with other detection methods.

Ultraviolet Detection: Ultraviolet light reflecting off the ground is observed and is analyzed to locate any recent disturbances in the ground. This method would only work for recently buried mines. It may also be used alongside other methods.[McFee, 25. Craib, 19]

1.1.5 Photon (X-Ray) Backscatter

Photon (very high frequency electro-magnetic waves) backscatter can provide a high resolution image of a buried object. A beam of X-rays sent into the ground is scattered by a buried object and collected and analyzed. Since the wavelength is much shorter than that of radar, the resolution of this method is much greater than for GPR

methods. However, it is not clear how this system would be implemented in the field and is still under investigation. X-ray equipment tends to be bulky and potentially dangerous to work with because of the high energy of the beams.[Craib, 20-21]

1.1.6 Acoustic and Seismic

There is current research in the detection of land mines using acoustic energy which is injected into the soil. The amount of energy reflected from buried target objects is recorded and analyzed. The acoustic impedance of a mine is significantly different from that of most soils. The practical imaging of objects is difficult because of naturally occurring inhomogeneities (holes and lumps) in the soil. The imaging requires significant computational power to reduce these false alarms. Also, a significant amount of time is required to adequately characterize the initial soil conditions. A practical system has yet to be devised.[McFee, 26-27]

1.1.7 Nuclear Magnetic Resonance (NMR), Nuclear Quadropole Resonance (NQR), Thermal Neutron Activation (TNA), Neutron Moderation

Although the principle of detection differs in these nuclear methods, the basic premise remains the same. The detection device searches for differences in the chemical composition between the explosive component of mines and that of the surrounding soil. These nuclear techniques analyze the air surrounding a mine and locate any explosive chemicals contained therein. For example, explosives contain a high concentration of nitrogen compared with normal soil.[McFee, 28]

In general, the detection rate significantly degrades when the soil becomes damp. The equipment required for this technology is currently very bulky and awkward to maneuver. It is uncertain how a field ready model would be constructed. Also, the NMR and NQR detectors cannot be used to detect metallic mines.[McFee, 28-30. Craib, 22]

1.1.8 Biosensors, Trace Explosive Detection (TED)

Dogs have been widely used with a high degree of success for their ability to smell explosives. The use of animals has shown some success in specific circumstances. In Afghanistan, dogs are used as an effective mine detection method. In general, the dogs must be very well trained and cared for to provide effective detection. This method does contain some element of danger since it is possible for the animal to accidentally detonate a mine.

South Africa also employs dogs in detecting land mines. Samples of air are collected while driving a protected vehicle over roadways with possible mines. These samples are taken back to the dogs for analysis. This method has met with some success. This method is meant to provide the location of the mine field rather than of individual mines.[McFee, 33. Craib, 21-22]

1.1.9 Mechanical Detection Methods

Buried mines represent a relatively abrupt change in the mechanical properties of the surrounding media (soil, sand, roots, etc.). Several different mechanical detection systems have been developed which utilize this fact. Some mechanical methods which have been proposed include the use of instrumented prods, accelerated surface erosion, and vibrating rollers. Most mechanical devices in use are primarily concerned with breaching a mine field rather than clearing one. Breaching involves the creation of a path through a mine field allowing passage of a military convoy. The plough and rotating flail methods are examples of these. All existing mechanical systems currently do not have the reliability necessary to ensure 100% mine detection.[McFee, 38. Craib, 23-25]

1.1.10 Hand Held Prodding

The hand held prod is the only method in current use for mine field clearance which has a near 100% detection rate. Personnel lie in a prone position prodding into the soil

at an angle of approximately 30 degrees with a two foot long steel prodder. When the operator feels he has encountered a solid object, the object is carefully removed and examined. This method is very dangerous and suffers from a high rate of false alarms caused by examining non-threatening objects such as rocks and debris. Instrumented prodders have been devised which can assist the operator by eliminating some false alarms. However, this is still a dangerous, time intensive search method.[McFee, 36]

1.1.11 Heated Probe Tip Prodders

Another interesting technique involves using the characteristic that plastic melts when heated. Once contact has been made with a plastic mine, a heated tip prodder could be observed to move into the plastic. This motion would not occur at the same rate in other objects such as rocks or tree roots.

1.2 Summary and Motivation of Current Work

Of the detection methods currently in use, only the hand prodder can provide near 100% mine detection. The danger, cost and time required by hand prodding make this method impractical for removing the vast majority of land mines laid in the field. The following discussion describes an automated mechanical method for land mine detection motivated by the hand prodder. The purpose of this method is to remove the danger from hand prodding while retaining the ability to determine the identity of hidden objects. To achieve this end, the vibration in a mechanized prodder, produced by contacting a hidden object, is recorded by a computer using an accelerometer mounted on the end of the prodder. The vibration information is broken down into several features which are indicative of the type of object struck. Using pattern recognition software in the form of an artificial neural network, the objects can be classified. The entire process is intended to be automated thus significantly reducing the risk to field personnel.

Automated prodding tests were performed on several objects buried beneath

The following chapters detail the process of striking objects, processing the vibration signals, and determining the success of identifying the objects. Chapter 2 discusses the theoretical model used to describe the dynamic behavior of a prodder impacting a hidden object. This model provides insight into the vibration characteristics of signals recorded by an accelerometer attached to the prodder. Chapter 3 provides a detailed account of the procedure and equipment used during testing. The following chapter explains how the data collected with the accelerometer was analyzed for the purpose of classification. It will be shown how the raw data was reduced into a series of quantifiable features used to identify the hidden object. Chapter 5 discusses the application of pattern recognition software to correctly identify the hidden object by analyzing these vibration features.

CHAPTER 2

MODELING OF OBJECT PRODDER IMPACT SYSTEM

In order to gain insight into the dynamic behavior of the prodder as it strikes an object, a mathematical model is required. This model will provide information about the types of vibration characteristics used to classify the objects. These characteristics are specific, quantifiable features intrinsic to the object type. In particular, the prodder and object system must be modeled to represent the contact observed through experimentation. This involves a transient analysis of the initial impact with the object. The model must be able to describe the behavior of the top of the prodder where the accelerometer is mounted during impact. The type of system considered is shown in Figure 2.1. This figure shows an AP land mine placed within a cavity in the ground and surrounded by loose soil. The prodder penetrates the loose soil and contacts the hidden mine.

The dynamic behaviour of an impacted object recoded with a load cell mounted on an impacting hammer has been studied.[Slavin, 1065] The study concluded that the frequency of vibration changed with the type of geometry of the specimen and the type of material used. Since most land mines have a fixed geometry, this should assist in classifying land mines apart from randomly sized debris. A study of the vibration characteristics of the solid prodder located in Appendix B agrees with this conclusion.

Another study on the dynamic behaviour of objects using an impacting instru-

ment is the study of human teeth and gum disease. An instrumented tapping rod lightly strikes a tooth and a vibration signal is recorded using an accelerometer. The tooth is struck repeatedly and the signals are averaged. The averaged signal was reduced to a single value which represents the health of the tooth and gum system. Several parameters of the time domain acceleration signal were examined in clinical trials.[Lukas, 65]

The current chapter describes models of the prodder and object system. These models are used to derive many of the features for object classification. The models are used to explain specific features observed during testing. The single degree of freedom model is used to define features in the time and frequency domain. Features can be expected to follow specific trends depending on an object's stiffness. A two degree of freedom system includes the effects of the soil on the prodder and object system.

2.1 Single Degree of Freedom Model

The simplest model of the prodder striking an object is the single degree of freedom (SDOF) mass spring system. The assumptions are discussed in the section below. The SDOF model is described in most elementary text books on mechanical vibrations.[Rao, Thomson] This model consists of a mass connected to a spring and a damper as shown in Figure 2.2.

2.1.1 SDOF Model Assumptions

In order to analyze the system, several assumptions must be made. The buried object is assumed to deform elastically as a linear one-dimensional spring k_{obj} when struck by the object. This value is meant to be an average value over the object's surface area. The prodder acts as a point mass m_p which undergoes deceleration due to object's restoring force. This assumes that the mass of the deforming mine is neglected. Referring to Figure 2.2, the distance the prodder travels after contacting the object

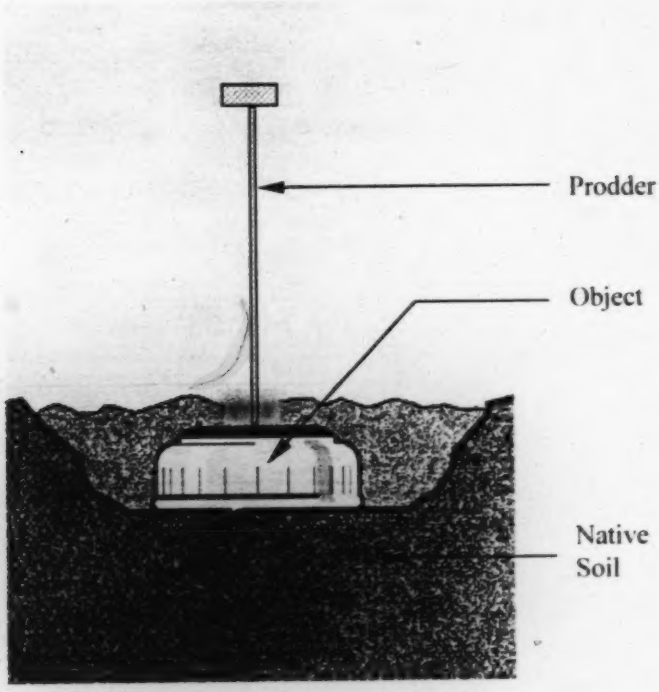

Figure 2.1: Schematic of the prodder and object system model.

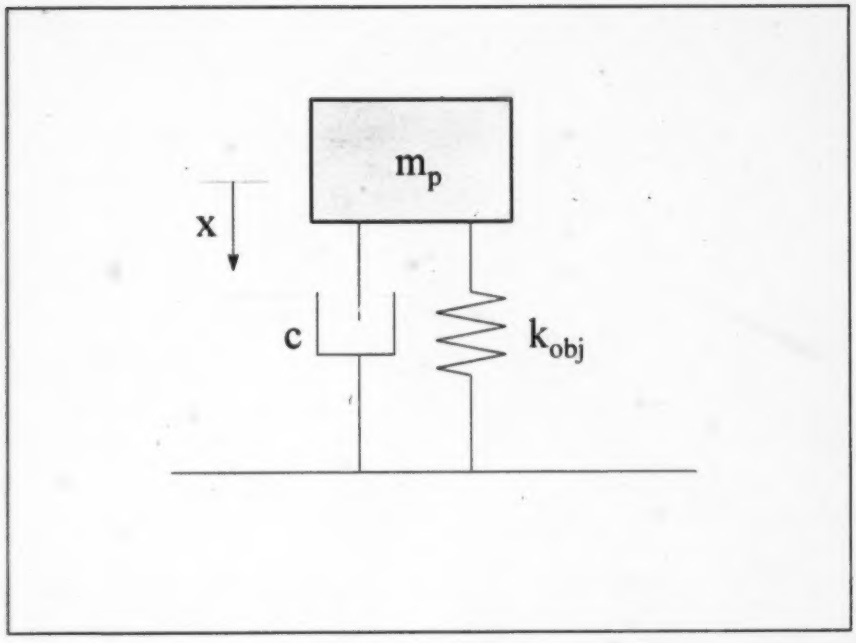

Figure 2.2: Single degree of freedom (SDOF) model of the prodder striking a compressible object.

spring is shown as the positive x direction. Analysis of the impulse caused by the prodder's impact reveals that the initial displacement immediately after contact will be zero, but it will have an initial velocity. This velocity will be v_0 which is caused by the firing mechanism as described in Chapter 3, Section 3.2. Because gravity is not considered an impulsive force (its magnitude is too small), the gravitational force will be ignored in this analysis. The soil is considered to provide damping proportional to the speed of the mass as $F_{damp} = c\dot{x}$. The value of c is dependent on the type and condition (wet, dry, baked, etc.) of the soil. It is assumed that the tip of the prodder will contact and remain rigidly attached to the object until the restoring force of the spring is zero. This means that the prodder will rebound and separate from the object at some point after the initial impact.

By performing a force balance on the mass, a single equation of motion can be derived:

$$m_p\ddot{x} + c\dot{x} + k_{obj}x = 0$$

There are specific features of this motion which are important in understanding the behavior of the system. These features occur in both the time domain and the frequency domain. Time domain analysis refers to examining the mass' acceleration features directly. Frequency domain analysis uses a mathematical technique known as a Fourier transform. This technique shows the relative contribution of various frequency sinusoids which are superimposed on one another to create the signal. The following subsections will discuss time and frequency domain analysis in more detail.

2.1.2 Time Domain Analysis and Features

The vibration behavior of the mass after impact is determined by the natural frequency of vibration of the system and the initial conditions (initial displacement and velocity) which cause the motion. The natural frequency of vibration for the SDOF case is $\omega_d = \omega_n\sqrt{1-\zeta^2}$ where:

$$\omega_d = \text{damped natural frequency}$$

$$\omega_n = \sqrt{\frac{k_{obj}}{m_p}} \text{ undamped natural frequency}$$

$$\zeta = \frac{c}{c_{cr}} \text{ damping ratio}$$

$$c_{cr} = 2\sqrt{k_{obj}m} \text{ critical damping value}$$

The prodder rebounds or bounces off the object after contact. As a result, only the first half-cycle of the sinusoidal vibration response is observed as shown in Figure 2.3. Figure 2.3 also shows two important time domain features: t_{wid} and A. The width of the pulse, t_{wid}, is the time which the prodder remains in contact with the object. The amplitude of the pulse, A, is the maximum acceleration experienced from the collision with the object. Its value is related to the initial velocity of the prodder just prior to impact. Another feature for classification is the integral, I, of the signal over the t_{wid} time period.

The amount of damping has a significant effect on the vibration characteristics. As the damping ratio ζ increases from 0 to 1, the width of the pulse (t_{wid}) increases, and A decreases. If the value of ζ is less than 1, the vibration is termed underdamped. With ζ equal to 1, the vibration is said to be critically damped. A ζ value greater than 1 is characteristic of an overdamped system. Both the underdamped and the overdamped cases are shown in Figure 2.4.

2.1.3 Frequency Domain Analysis and Features

System responses may also be analyzed in the frequency domain by converting the original vibration pattern into a summation of sinusoids. The Fourier transform is a commonly used mathematical technique for determining the frequency and amplitudes of these sinusoids.[Lynn, 211-246] The superposition of these sinusoids at the correct amplitudes and phases will reconstruct the original signal. Therefore the original signal can be represented by the characteristics of its composite sinusoids. The

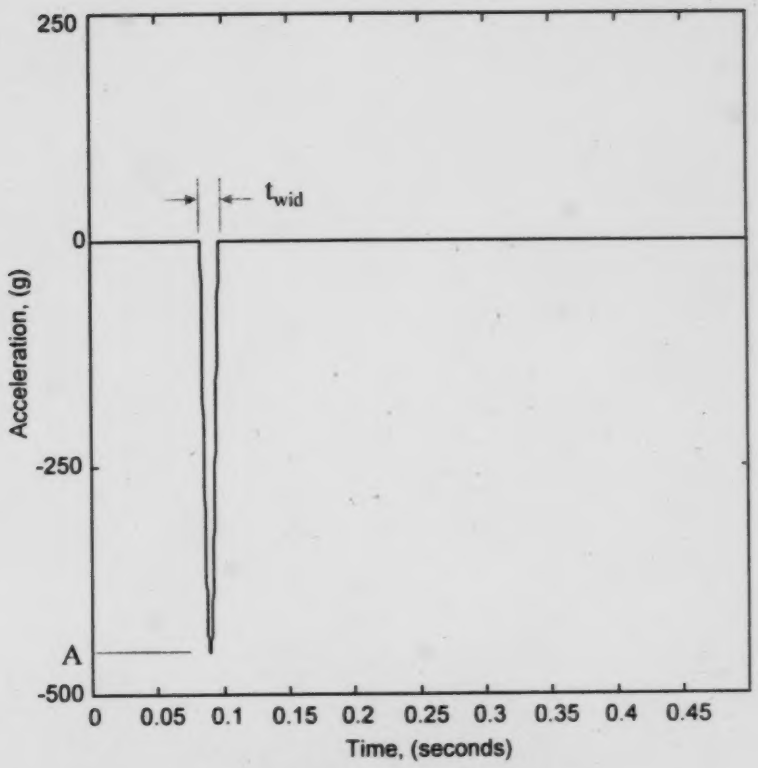

Figure 2.3: A single degree of freedom model vibration pattern. Only the first half cycle of the response is shown. This mimics the behavior of the prodder bouncing off the object after contact. Also shown are the time domain features of t_{wid} (the width of the pulse) and A (amplitude of the pulse).

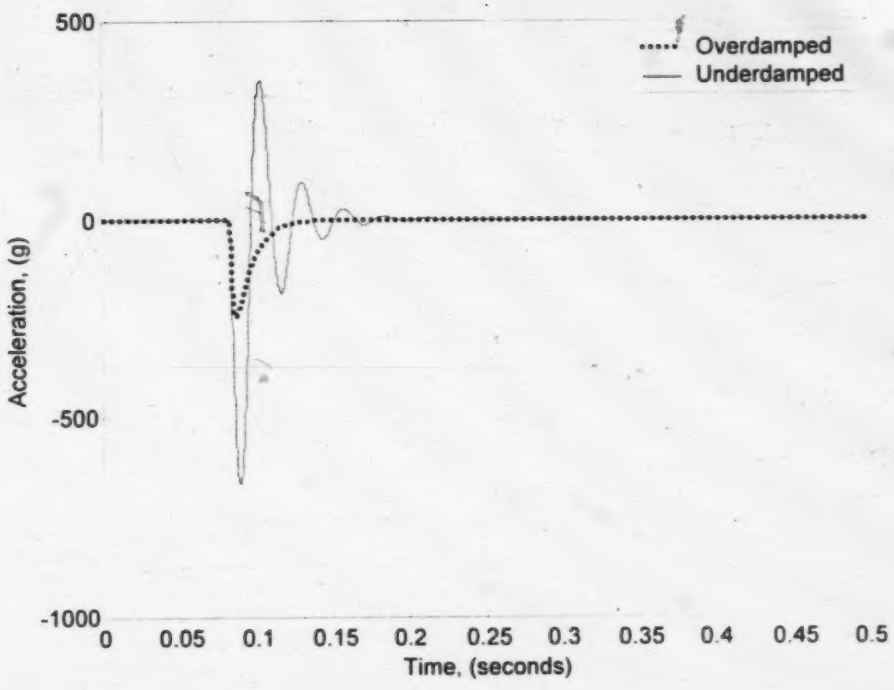

Figure 2.4: The time domain vibration response of a SDOF model with damping using ζ values of 0.2 and 1.5.

frequency, phase and amplitude of the sinusoids are the frequency domain characteristics of the original signal. Time domain signals $h(t)$ are converted in this way to frequency domain signals $H(f)$.

The amplitudes of the sinusoids are of particular interest in frequency domain analysis. The power spectrum is often used to visualize these amplitudes. It is obtained by squaring the frequency domain signal $H(f)$. A SDOF system with no damping has one natural frequency. The power spectrum should consists of a single frequency ω_n centered at that frequency. For a SDOF system with damping, however, the frequency domain is more complicated. Figure 2.5 shows the power spectrum of an underdamped and an overdamped system, $\zeta = 0.2$ and 1.5. The single frequency has changed to a wider, smeared-out spectrum with a peak value shifted to the left. The shifting increases in magnitude as the value of ζ increases to 1. For $\zeta > 1$, the peak value reaches zero.

2.1.4 SDOF Results

Table 2.1 contains the values of features determined from the acceleration of the prodder in a SDOF system striking an object which has the same stiffness as a VS-50 AP mine.

The time domain features t_{wid}, A, and I shown in Table 2.1 are the same as the features defined in Section 2.1.2. The average acceleration amplitude contained in twelve frequency bands are also provided. The feature f_{peak} represents the largest amplitude found in the frequency domain.

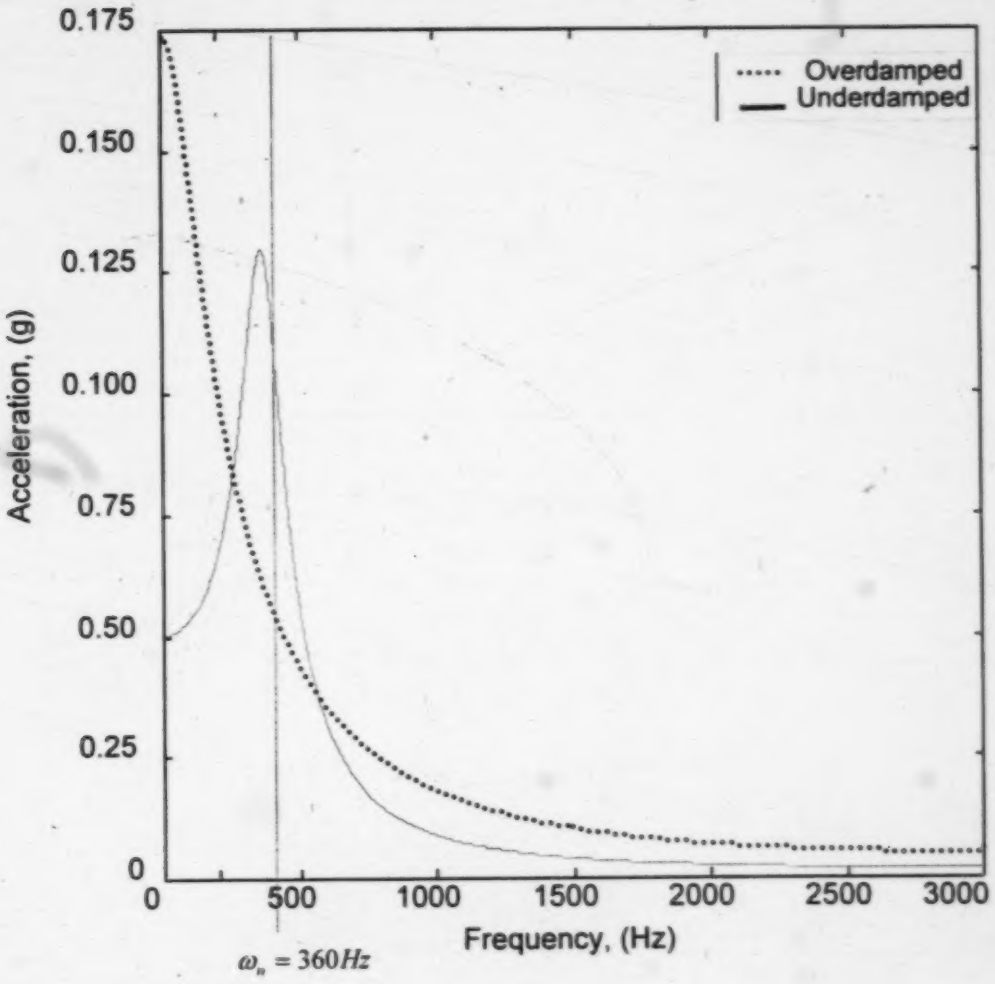

Figure 2.5: The frequency domain response of SDOF system with $\zeta = 0.2$ and 1.5.

Table 2.1: SDOF features using VS-50 AP mine stiffness.

Feature	**Velocity**			
	0.5 m/s	**1.0 m/s**	**2.0 m/s**	**5.0 m/s**
t_{wid} (ms)	12.67	12.67	12.67	12.67
A, Amplitude (g)	12.43	24.86	49.72	124.3
I, Integral ($g \times s$)	0.102	0.204	0.408	1.02
F(1-25 Hz) (g)	0.038	0.157	0.606	3.79
F(26-50 Hz)	0.027	0.107	0.428	2.67
F(51-75 Hz)	0.012	0.046	0.185	1.15
F(76-100)	0.003	0.010	0.040	0.252
F(101-200)	0	0	0.002	0.011
F(201-300)	0	0	0	0.002
F(301-400)	0	0	0	0
F(401-600)	0	0	0	0
F(601-1000)	0	0	0	0
F(1001-1500)	0	0	0	0
F(1501-2000)	0	0	0	0
F(2001-3001)	0	0	0	0
f_{peak} (g)	0.0415	0.166	0.665	4.154

Measured values for m_p, m_{obj}, k_{obj} and k_{soil} are found in Appendix A. For the VS-50 AP mine trigger pad, the natural frequency based on a SDOF system model is 38.8 Hz. This corresponds to a period of about 26 milliseconds. A half of a period would then have a time span of almost 13 ms. This is the expected amount of time that the prodder would take to rebound off the object and become separated.

The SDOF system shows that the amplitudes of the time and frequency domain features, with the exception of t_{wid}, are strongly influenced by the initial velocity of

the prodder. The feature t_{wid} is influenced by the system natural frequency which is proportional to the square root of the object stiffness.

To reduce the sensitivity to changing velocities, the acceleration signal may be normalized by dividing the signal by the maximum amplitude. Table 2.2 shows the features after normalizing the time domain signals. The values of each feature remain constant. Since the undamped SDOF system contains only one frequency component, the features are directly proportional to the initial velocity of the prodder.

Table 2.2: SDOF features after normalizing the time domain signals.

Features	**Values**
$t_{wid}(ms)$	12.67
A, Amplitude $(\frac{g}{g_{peak}})$	1.0
I, Integral $(\frac{g}{g_{peak}}s)$	0.00820
F(1-25 Hz) $(\frac{g}{g_{peak}})$	2.45×10^{-4}
F(26-50)	1.73×10^{-4}
F(51-75)	0.163×10^{-4}
F(76-100)	0.0069×10^{-4}
F(101-200)	0.0010×10^{-4}
F(201-300)	0.0001×10^{-4}
F(301-400)	0
F(401-600)	0
F(601-1000)	0
F(1001-1500)	0
F(1501-2000)	0
F(2001-3000)	0
f_{peak} $(\frac{g}{g_{peak}})$	2.69×10^{-4}

The variability in the frequency domain features is removed by normalizing the initial signal prior to signal processing. The time domain feature of t_{wid} is unaffected

by normalization. By definition, the amplitude A will be 1.0 after normalization takes place. While the variability in the signal due to velocity changes is reduced, the information about the initial signal held in the features is also reduced.

2.2 2DOF System, Compressible Soil

The acceleration data collected from striking objects is more complicated than the signals obtained using a SDOF model since the shapes are more complicated than that of a pure half sine wave. The shape of the VS-50 AP mine acceleration data shows that there are two peaks within the main signal pulse. As a result, the features in the time and frequency domain cannot be described sufficiently by a SDOF model. A two degree of freedom system (2DOF) introduces a second peak within the main pulse.

The previous SDOF system assumed that the soil was solid and did not contribute to the vibration of the prodder except as a damping mechanism. A compressible soil would allow the object to move as the prodder impacts the soil beneath the object. The simplest model for the soil is to consider it to be a one dimensional spring beneath the object. As shown in Figure 2.6, the object and the soil have associated stiffnesses k_{obj} and k_{soil}. The object sitting in the soil has a mass m_{obj}, and the prodder has a mass m_p as in the SDOF case. The displacement of the prodder is x_1; displacement of the object is x_2. The positive direction is considered down.

Analysis of the force balance on each of the masses in this system provide the equations of motion. In matrix form, the equations are as follows:

$$[m]\{\ddot{x}\} + [k]\{x\} = \{0\}$$

The mass matrix is defined for this system as:

$$[m] = \begin{bmatrix} m_p & 0 \\ 0 & m_{obj} \end{bmatrix}$$

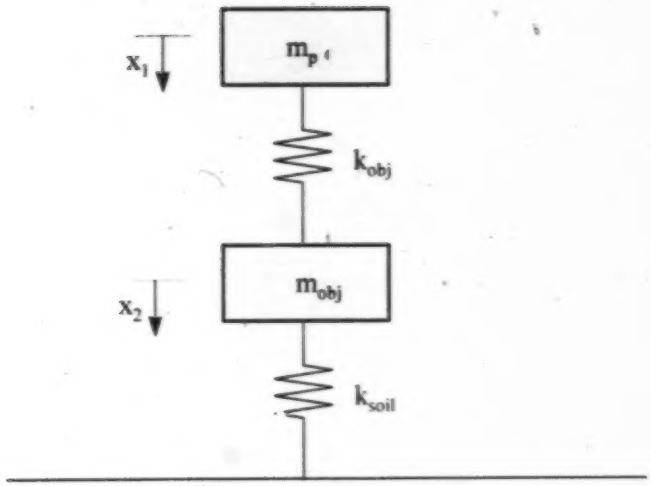

Figure 2.6: 2DOF model of the prodder and object impulse system.

and the stiffness matrix is:

$$[k] = \begin{bmatrix} k_{obj} & -k_{obj} \\ -k_{obj} & k_{obj} + k_{soil} \end{bmatrix}$$

In the 2DOF model, secondary peaks are introduced into the pulse of the signals when the spring constant k_{obj} is of the same order of magnitude as the soil spring constant k_{soil}. As the soil spring constant increases, the secondary peaks disappear. When $k_{soil} \gg k_{obj}$, the 2DOF model approaches the single pulse half sine wave as found in the SDOF system. Given the soil and spring stiffness of the VS-50 mine trigger as shown in Appendix A, the two natural frequencies of the 2DOF model are $\omega_1 = 33.8$ Hz and $\omega_2 = 68.6$ Hz. A more detailed analysis of the 2DOF model is available in Appendix B.

One of the difficulties during modeling was the determination the spring constant of the soil. The soil stiffness of 26.1 kN/m used in this model was determined experimentally by pressing on a 254 mm diameter disk onto the soil. For the 90 mm diameter VS-50 mine, this makes the soil stiffness k_{soil} equivalent to 3.3 kN/m. This values is assumed to be constant. However, the soil conditions during testing were continually changing as the mine was repositioned and moved. For the purposes of modeling, a constant value for k_{soil} of 3.3 kN/m was used.

Using a constant soil stiffness and using the properties of the VS-50 AP mine, signal features in the time and frequency domain were determined. Table 2.3 contains features obtained using several different initial velocities. As in the case of the SDOF model, the features were normalized by dividing each signal by the peak amplitude prior to deriving the feature values. The features remain similar in magnitude to the SDOF values.

Table 2.3: 2DOF model features.

Features	**Initial Velocity**			
	0.5 m/s	**1.0 m/s**	**5.0 m/s**	**200 m/s**
t_{width} (ms)	10.83	10.67	10.67	10.67
I, Integral ($\frac{g}{g_{peak}}s$)	0.00694	0.00690	0.00687	0.00686
F(1-25 Hz) ($\frac{g}{g_{peak}}$)	1.79×10^{-4}	1.77×10^{-4}	1.75×10^{-4}	1.75×10^{-4}
F(26-50)	1.40×10^{-4}	1.39×10^{-4}	1.38×10^{-4}	1.38×10^{-4}
F(51-75)	0.776×10^{-4}	0.777×10^{-4}	0.777×10^{-4}	0.777×10^{-4}
F(76-100)	0.286×10^{-4}	0.290×10^{-4}	0.294×10^{-4}	0.295×10^{-4}
F(101-200)	1.73×10^{-6}	1.79×10^{-6}	1.84×10^{-6}	1.86×10^{-6}
F(201-300)	0.10×10^{-6}	0.0011×10^{-6}	0.11×10^{-6}	0.11×10^{-6}
F(301-400)	0.02×10^{-6}	0.02×10^{-6}	0.02×10^{-6}	0.02×10^{-6}
F(401-600)	0.01×10^{-6}	0.01×10^{-6}	0.01×10^{-6}	0.01×10^{-6}
F(601-1000)	0	0	0	0
F(1001-1500)	0	0	0	0
F(1501-2000)	0	0	0	0
F(2001-3000)	0	0	0	0
f_{peak} ($\frac{g}{g_{peak}}$)	1.92×10^{-4}	1.90×10^{-4}	1.89×10^{-4}	1.88×10^{-4}

Comparisons were made with results of the 2DOF model with actual signals obtained from striking the objects. An overlay of the Runge-Kutta solution of the AP mine VS-50 2DOF model and the VS-50 vibration signal is found in Figure 2.7. The resulting vibration signal from the 2DOF model closely matches the experimental pulse shape, but it does not represent the secondary peaks within the pulse of the object signal. Assuming that the values k_{soil} and k_{obj} are approximately correct, then it is reasonable to assume that the soil does not introduce the secondary peaks in the pulse of the experimental signal.

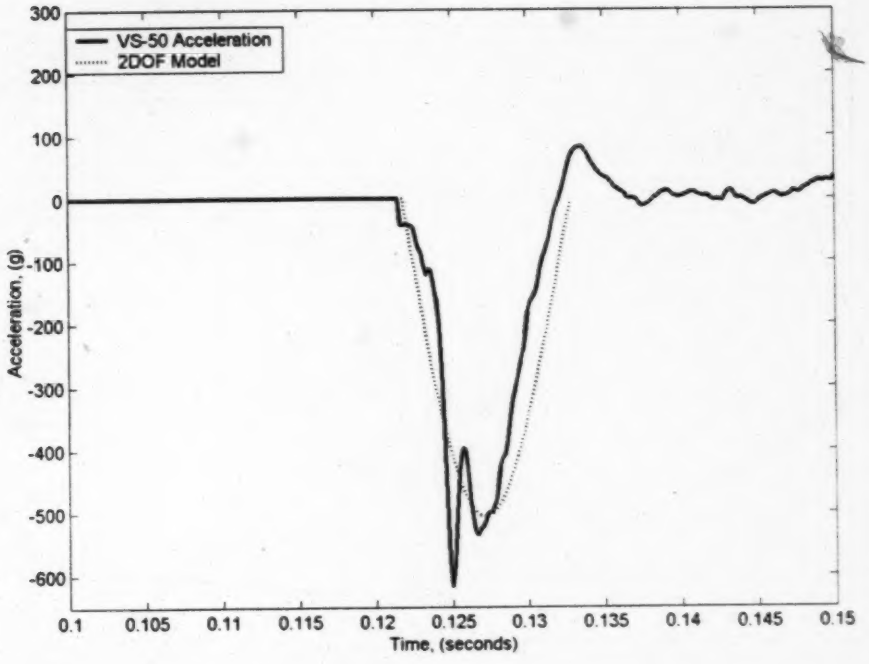

Figure 2.7: Processed time signal output from accelerometer as prodder strikes the VS 50 antipersonnel mine. Only the first half pulse is plotted.

During the test procedures described in Chapter 3, the AT mines were placed very low in the container and soil was distributed over top. As a result, it is unlikely that there was enough soil underneath the AT mines to provide a significant flexure. Thus, it may be assumed that k_{soil} should be modeled such that $k_{soil} \gg k_{obj}$. When the soil conditions are such that $k_{soil} \leq k_{obj}$, then the soil has very little influence in the vibration pattern observed at the prodder's location.

It is worth mentioning that during testing, t_{wid} remained relatively constant despite varying soil conditions such as compacted soil, stirred loose soil, or wet soil. Since the object's t_{wid} did not change significantly, it suggests that the object itself may be contributing to the multiple peaks observed in a signal pulse.

2.3 Conclusions of Modeling

The goal to modeling is to gain an understanding of the dynamic behavior as the prodder contacts objects. The SDOF model provides a useful first approximation to the contact observed through experimentation. The half sinusoid pulse provides several quantifiable features in the time and frequency domain. In addition, knowledge of the relative stiffnesses of the objects tested can be used to predict the values of these features. Unfortunately, the SDOF model does not completely describe the shape of the observed signal. Secondary peaks are observed within the intial signal pulse.

In an attempt to further model the observed signals, a 2DOF model was created that included the compressibility of the soil beneath the objects. This model did not show additional peaks within the initial pulse. This 2DOF model indicates that the soil does not introduce the additional peaks in the initial pulse. Since the prodder is considered incompressible, this means that the secondary peaks are inherent properties of the objects themselves. Each of the different objects tested have different vibration signals.

CHAPTER 3

TEST EQUIPMENT AND PROCEDURES

This chapter describes the test equipment and procedures used to collect vibration data from the contact of the prodder with various buried objects. Through an automated process, a $\frac{1}{4}$ inch diameter steel prodder was brought into contact with a buried object. The vibration in the prodder produced by this contact was recorded by an accelerometer.

3.1 Data Acquisition Hardware and Software

Data acquisition and control was achieved using the National Instruments AT-MIO-16E acquisition card and using LabVIEW 4.0 software. The data acquisition board has 16 single ended analog input channels with a multiplexed sampling rate of 100,000 samples per second. The board also has 8 digital I/O channels. The digital output channels were connected to solid state relays which toggled solenoid valves on and off. In this way, control of the test procedure was completely automated.

LabVIEW software provided the triggering ability necessary to capture the transient vibration signature of each target struck by the prodder. LabVIEW is a graphically based computer language specifically designed for use with National Instruments' hardware.[National Instruments] Using LabVIEW, the control sequence and the data acquisition parameters were set.

By analyzing the frequency spectrums of the various objects, the vast majority

of the spectral energy was located below 3000 Hz. As a result, the sampling rate for accelerometer data acquisition was set to 6000 Hz. An anti-aliasing Krone-Hite lowpass filter was set at 3000 Hz based on the Shannon sampling criteria.

The accelerometer used was a uni-directional PCB Piezotronics model Q353B13 which has a sensitivity of 5.44 mV/g and a linear frequency range from 1 to 10000 Hz. This accelerometer was threaded into the top of the steel prodder. The specifications of this device are found in Appendix C. Smaller range accelerometers were tried (50 and 100 g ranges), but the acceleration experienced by the prodder was seen to exceed these limits. Solid state piezoresistive accelerometers manufactured by IC Sensors (model 3032) did not withstand the rigors of the test procedures. Advantages of this type of accelerometer are low cost, light weight design, and a small size. However, after several hundred tests, the pins attached to the electronics at the base of the accelerometer would shear off. The PCB Piezotronics model accelerometer is more rugged in design. It is more expensive, but is similar in size and weight to the IC Sensors accelerometer.

The vibration data was recorded into a datafile for analysis. Analysis was performed using Matlab 5.0 software. Matlab was chosen for its programming ease and many built-in signal processing tools such as filters and Fourier transforms.

3.2 Apparatus and Procedure

All tests were performed in a wooden box constructed of $\frac{1}{2}$ inch plywood with dimensions 39 cm by 39 cm by 31 cm deep. The box was filled with 16.5 liters of soil. The soil material tested was a clayey silt of low plasticity that is locally known as "Devin silt". Additional details about this material have been reported by Konrad.[Konrad] For wet soil tests, 1.65 liters (10% volume) water was added and stirred into the soil until thoroughly mixed. Buried tests were conducted in both wet and dry soil conditions. AP mines and the wood and steel objects were placed 30 mm under the soil. Due to the constraints of the box used and the amount of soil available, AT mines

were placed at the bottom of the wooden box and covered in 130 mm of soil.

3.2.1 Apparatus

The prototype used to investigate object vibration classification is shown in Figure 3.1. The design consists of a metal frame, a large pneumatic cylinder, a spring firing mechanism, various solenoid valves, and a prodder with an attached accelerometer. The design allows the prodder to contact objects at various angles and soil burial depths. The large cylinder provides the means to move the prodder through different depths of buried soil. Attached to the end of this cylinder is the spring firing mechanism containing the prodder and accelerometer.

The main cylinder would be used to lower the prodder into contact with a test object. If no object was encountered, the cylinder would retract and the prodder or object would be repositioned. Once an object was contacted, the main cylinder would hold the prodder and firing mechanism above the object. With the prodder held in place above an object, several strikes in succession could be made in the same region of the object. The number of strikes in succession were 2, 5, 10 and 20.

3.2.2 Striking Method

The prodder was fired at the test object to create an impulse vibration signal. The custom-designed spring firing mechanism provided a consistent velocity for the prodder. As seen in Figure 3.2, the mechanism uses a small pneumatic cylinder to move a hook up and down. On the hook's down stroke, it passes over a pin which is connected orthogonally to the side of the prodder. This pin moves within a slot in the prodder's housing. As the hook moves upward, it pulls on this pin and lifts the prodder. As the prodder lifts, it begins to compress a spring until the hook rides over a lip in the housing which allows the pin to slip underneath the hook. The prodder fires at approximately the same velocity each time. This firing mechanism allows the prodder to be relatively uncoupled from the rest of the apparatus. The limited resistance of

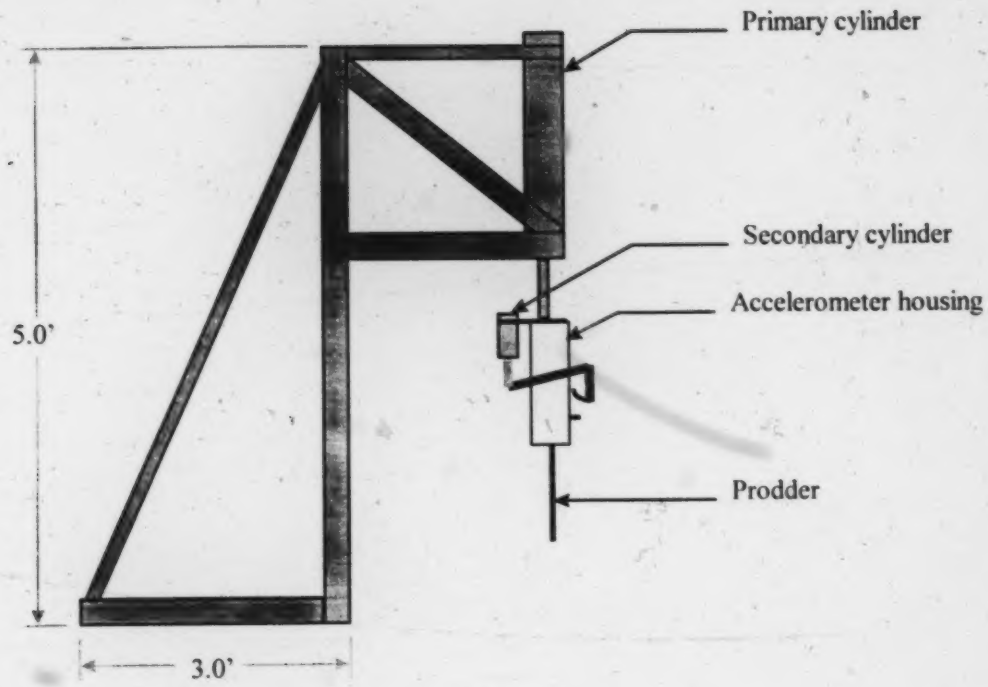

Figure 3.1: Schematic drawing of the apparatus use during testing.

this method means that energy lost due to friction is minimized.

3.2.3 Test Objects

Tests were performed on various known objects. These included five plastic landmines, a block of wood, and a piece of steel. The landmines used in this study were loaned from DRES (Defense Research Establishment Suffield) military establishment in Suffield, Alberta. The mines were the AP mines: VS 50, and the PMA 1A; and the AT mines: TMA-4, TMA-5A, and VS 2.2. A full description of the dimensions of these objects is available in Appendix A.

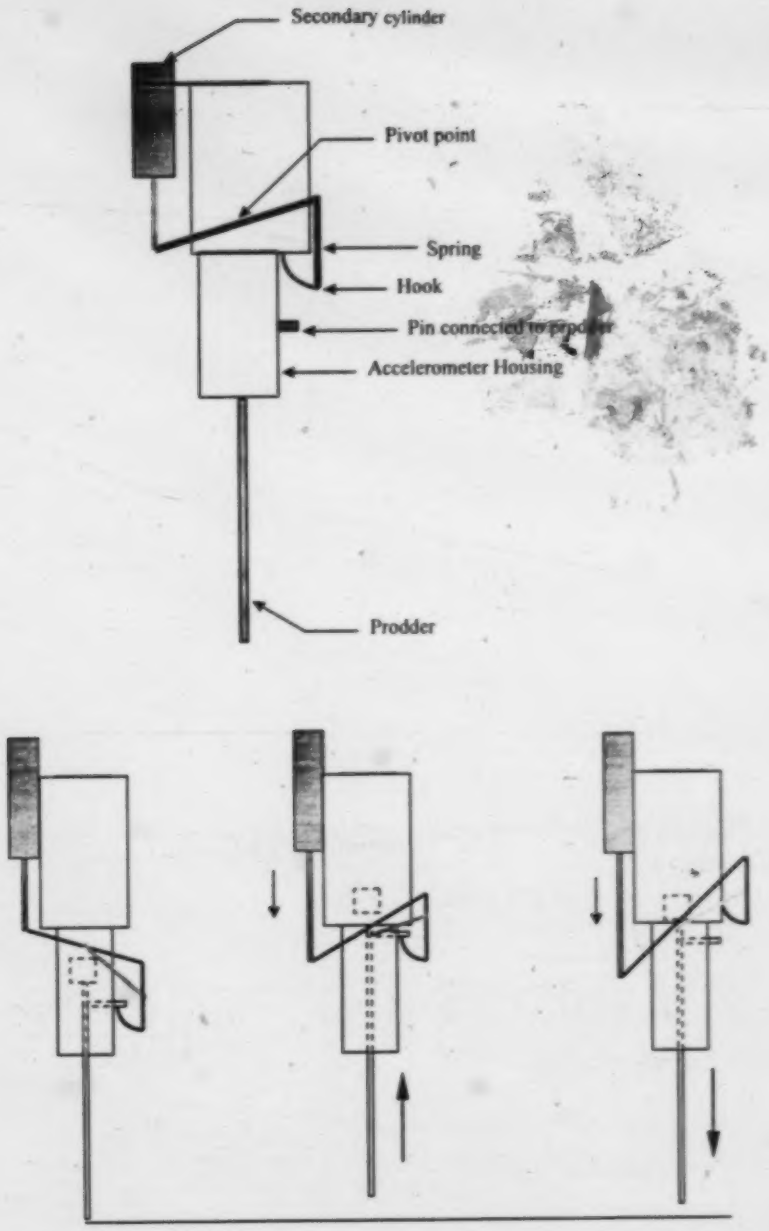

Figure 3.2: Prodder firing mechanism with hook that lifts the prodder.

CHAPTER 4

DATA PROCESSING AND FEATURE EXTRACTION

This chapter discusses how the vibration signatures of various objects were analyzed for the purpose of classification. The vibration signal contains information about the properties of the object struck by the prodder. The specific features of the vibration signal which distinguish one object from the next are discussed.

This chapter describes how the raw data recorded with the accelerometer from each strike was used to extract features used in ALN pattern recognition. The raw data was adjusted to capture only the pertinent information. Using the cleaned signals, features were extracted from the time and frequency domains. How these features are used for pattern recognition are discussed in the following chapter.

4.1 Raw data

The vibration signals were obtained by striking an object with a $\frac{1}{4}$ inch steel prodder through the automated process discussed in the Chapter 3. These signals were stored into data files for analysis. From these data files, features were examined which could be used to identify each object as unique. The bulk of this analysis was done using Matlab software.

Figure 4.1 shows the voltage output recorded from the accelerometer after striking a VS-50 AP mine. This is typical of the raw data provided by the accelerometer without modification in any way. The signal includes the data from the hook pulling

the prodder and release of prodder prior to striking object (as described in Chapter 3). Noise from external sources may also be present in the signal. In order to be useful, relevant information must be separated from non-relevant information. The following section will describe the ways in which pertinent information was extracted from the raw data, and how noise was reduced in the signals.

4.1.1 Initial Noise Removal

The first step in cleaning the signal prior to analysis was to remove the initial hook release portion recorded by the accelerometer. The signals were also truncated to remove noise after the initial transient event. Figure 4.2 shows the same data as shown in Figure 4.1 after this action has been performed.

The truncation and removal of the hook release portion of the signal was done with LabVIEW just after the object was struck on each run. If the strike missed the intended target, no information would be recorded after the hook release. These events would be removed from the test set and the strike would be repeated. Once a pre-determined number of strikes were successfully recorded, the data from these strikes would be saved in a data file for further analysis. Zeroes were also added before and after the signal (zero padded) to improve the frequency domain resolution.

4.1.2 Averaging a Series of Prodder Strikes

In order to aid in noise reduction, truncated signals were averaged. Ten strikes of the prodder were made in succession on a particular region of an object. A computer algorithm developed using Matlab was used to average the signals (see Appendix C). Each signal was positioned to line up the peak amplitude positions. The result of the signals thus averaged was a single signal as shown in Figure 4.3.

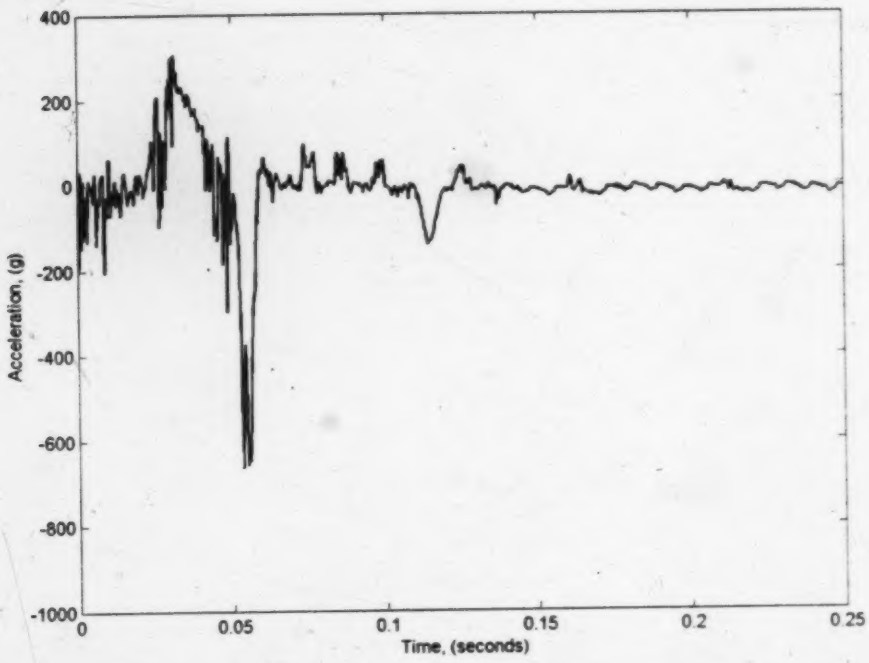

Figure 4.1: Time signal output from accelerometer as prodder strikes the VS 50 antipersonnel mine.

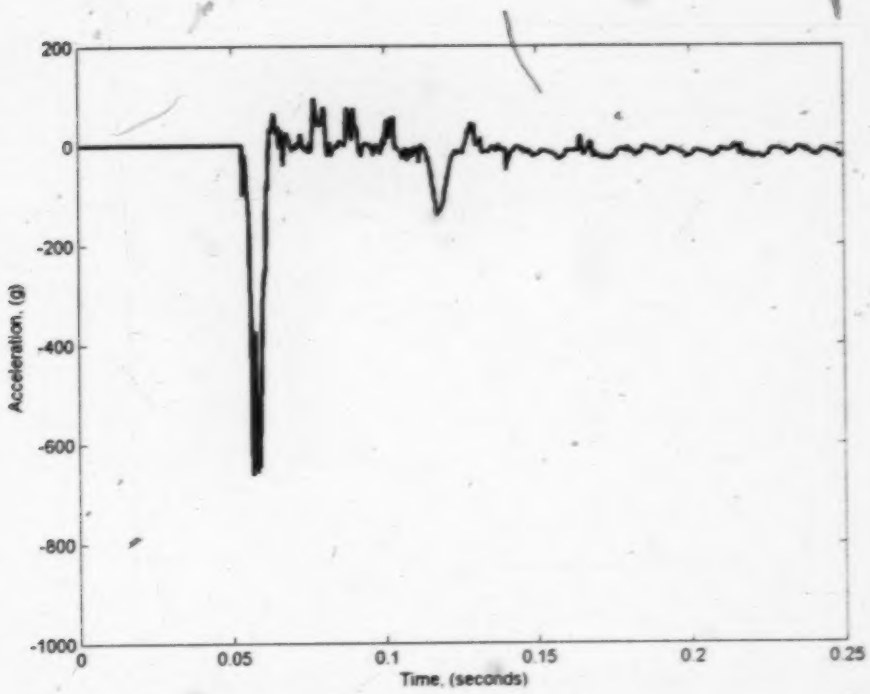

Figure 4.2: Processed time signal output from accelerometer as the prodder strikes the VS 50 antipersonnel mine.

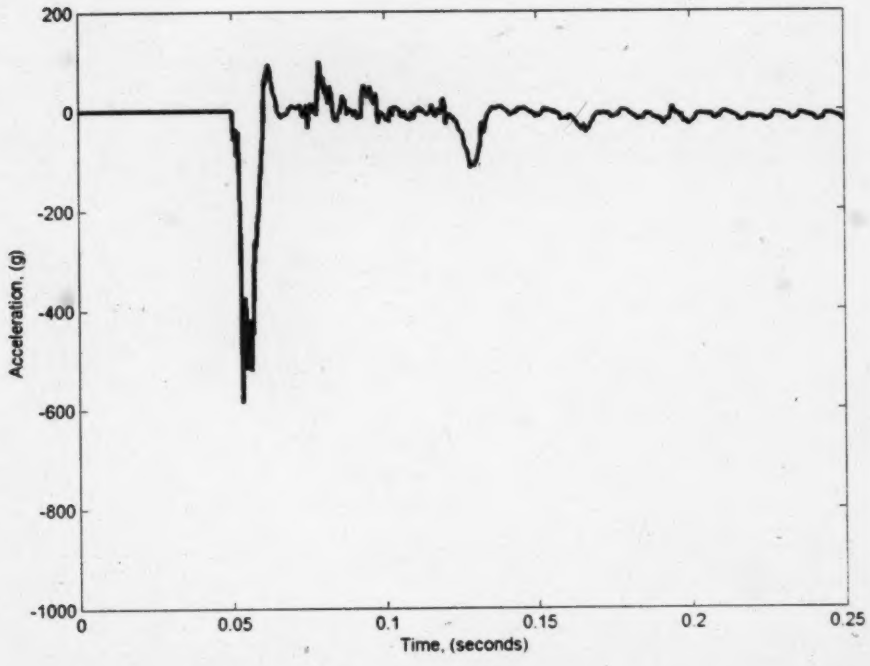

Figure 4.3: Averaged time signal output from the accelerometer as the prodder strikes the VS-50 AP mine using 10 strikes in succession on a specific region of the mine.

4.2 Signal Feature Extraction

During the averaging process, time and frequency domain features were obtained from the signals.

4.2.1 Time Domain Features

The time domain features are the same features as described in section 2.12. This includes the largest absolute acceleration of the signal (A), the time width of the main pulse of the signal (t_{wid}), and the integral of the main pulse (I). The main pulse refers to the time that the signal spends below a threshold voltage level. The main pulse surrounds the minimum value of the signal. The threshold for determining the starting and stopping times of the pulse were determined using trial and error. The pulse area feature is calculated by summing the values of the time domain signal within the main pulse. The Matlab program to perform this function is provided in Appendix C.

Each feature of an object was averaged during this ten strike averaging procedure described earlier. At the same time, the standard deviations for each feature were determined. Thus, for the time domain, a total of six features were used.

4.2.2 Frequency Domain Features

After the signals of the objects were averaged, frequency domain characteristics were obtained. A Fourier transform of the time domain signal was determined. The frequency domain resolution is 1 Hz given that the sample length is 6000 data points, the sampling rate was 6000 Hz. The frequency domain signal for the averaged VS-50 AP mine is shown in Figure 4.4. The frequency domain was divided into twelve unequal segments. The twelve segments were chosen to adequately break up the frequency domain and provide consistent features. The frequency domain was observed to be dominated by low frequencies. The twelve segments concentrate on the low

frequency range of the vibration signals. The frequency amplitudes in each segment were averaged, and this average value was used as a feature. The maximum frequency component was also used as a feature. Thus a total of thirteen frequency domain features was used for each signal.

4.3 Example of Feature Values

By way of example, the average of ten VS-50 AP mine signals will be used to assist in describing these features. Table 4.1 shows the time and frequency domain features of the average of ten VS-50 AP mine signals. The vibration features including t_{mid}, I, A, and their standard deviations, and the frequency bands were obtained from the data files collected during testing. After obtaining the features, each feature and the object associated with those features was saved in a new database. This database was the raw data upon which the pattern recognition software learned to associate the hidden objects with the vibration features.

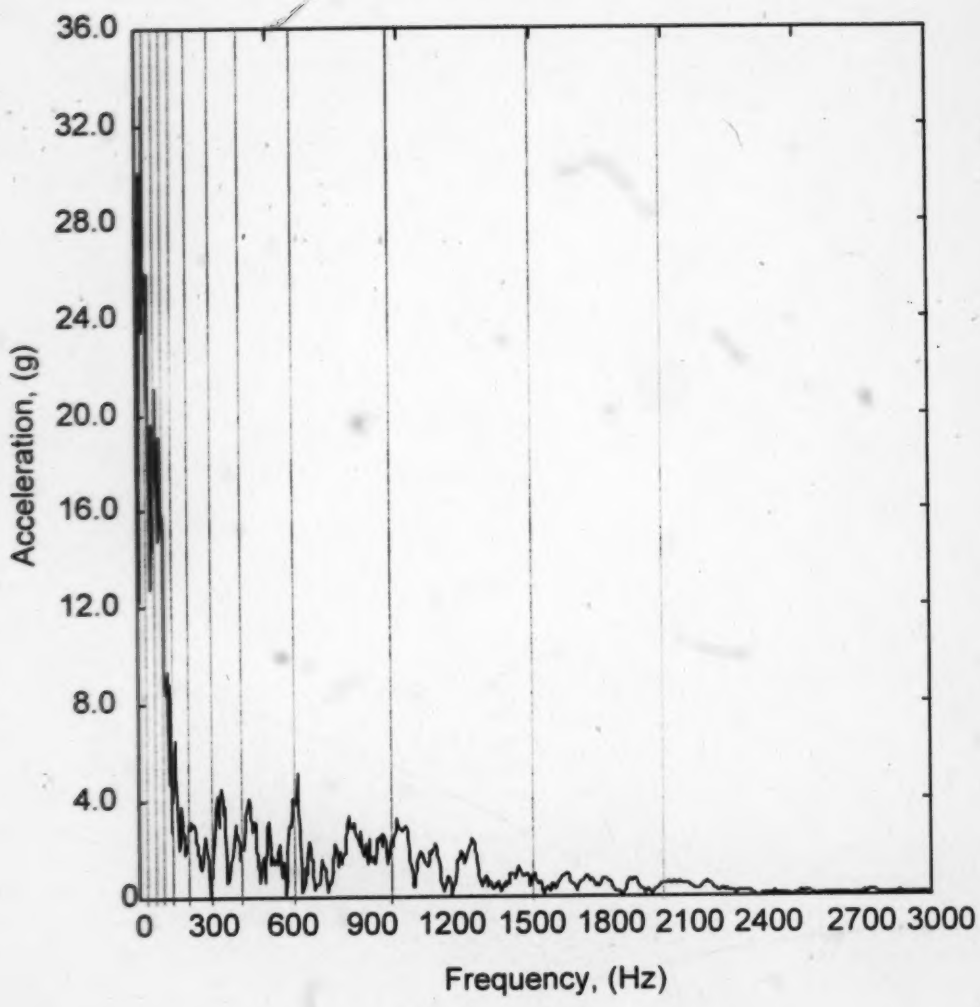

Figure 4.4: Frequency domain features of the averaged time signal of the VS-50°AP mine.

Table 4.1: Features extracted from 10 averaged VS-50 AP mine signals

Feature	**Value**
t_{wid} (s)	0.008467
A, Amplitude (g)	617
I, Integral ($g \times s$)	0.2783
F(1-25 Hz) (g)	4.79
F(26-50 Hz)	2.87
F(51-75 Hz)	1.87
F(76-100)	0.753
F(101-200)	0.134
F(201-300)	0.0088
F(301-400)	0.0145
F(401-600)	0.0116
F(601-1000)	0.0033
F(1001-1500)	0.0003
F(1501-2000)	0.0001
F(2001-3001)	0
f_{peak} (g)	717

4.3.1 Feature Extraction Results

From the time domain, the features t_{wid}, I, A and their standard deviations were calculated. Figure 4.5 is a scatter plot of the feature t_{wid} and the object from which t_{wid} was calculated. This plot shows the value of the feature t_{wid} as determined from the signals of each of the different classes of objects tested. If the prodding tests could be repeated exactly on the same spot on an object, one would expect that value of t_{wid} for that object would be a single value. As can be seen, t_{wid} takes on a range

of values instead of a single value. Also, two or more different objects (for example VS-50, TMA-4, wood) have t_{wid} values which are approximately the same. Because of this overlap, it would be impossible to identify an object with certainty using the feature t_{wid} exclusively. It is for this reason that several features are required for classification.

In contrast to Figure 4.5, Figure 4.6 displays the calculated value of the feature $\sigma_{t_{wid}}$ along with its associated object class. No clear patterns can be found using this feature alone. Some information is available from even this type of feature, however. There is a difference between the amount of variation in $\sigma_{t_{wid}}$ between the objects VS-50 and TMA-4. This difference may be used to help distinguish the two classes.

In the frequency domain, most of the energy is concentrated below 1000 Hz. The stiffer the object, the larger the higher frequency components of the signal. This agrees with the SDOF with damping theory. The peak frequency of the signals changes was observed to change in amplitude and frequency from one strike to the next in contrast to the constant value predicted by the theory.

4.4 Summary of Feature Extraction

The raw signals from the accelerometer need to be processed before they can be classified. First noise from the initial firing of the prodder onto the object must be removed. To further reduce the influence of noise, several signals are averaged together prior to extracting features. This requires that the signals are lined up by their peaks and reduced to a single signal.

There were a total of six time domain and thirteen frequency domain features are extracted from each signal. Thus the complex acceleration signal is reduced into nineteen features that describe that signal. These features are stored in a database to be used in classifying the objects. A complete list of the object features can be found in Appendix D. The averaged acceleration signals are shown in Appendix E.

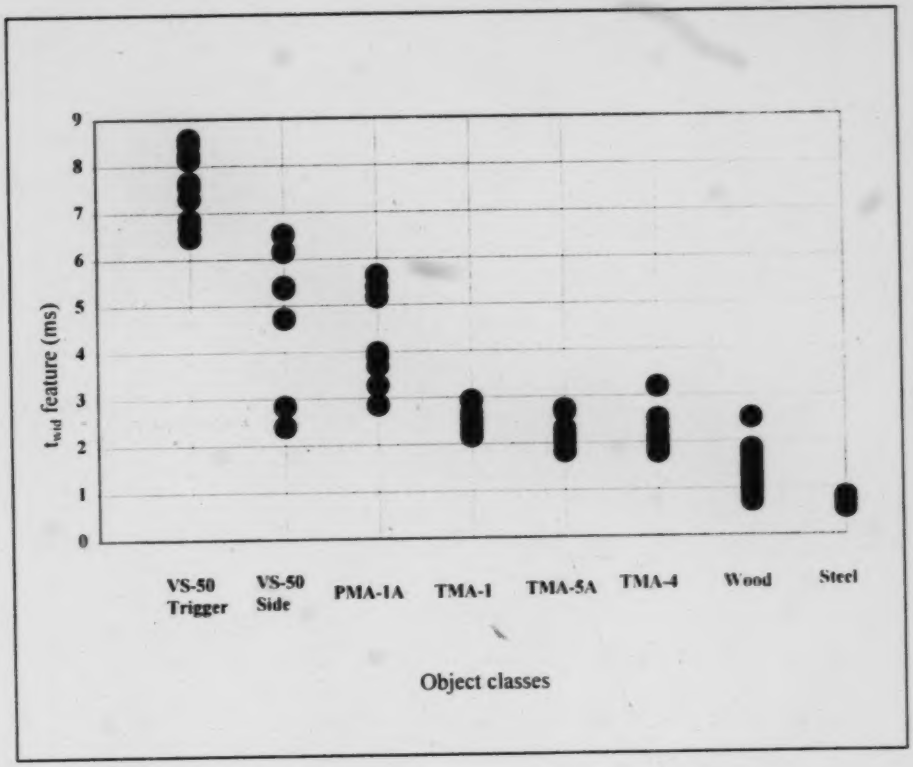

Figure 4.5: The t_{wid} feature variable for each object class. Each data point represents the average of ten strikes in succession on a specific region of an object.

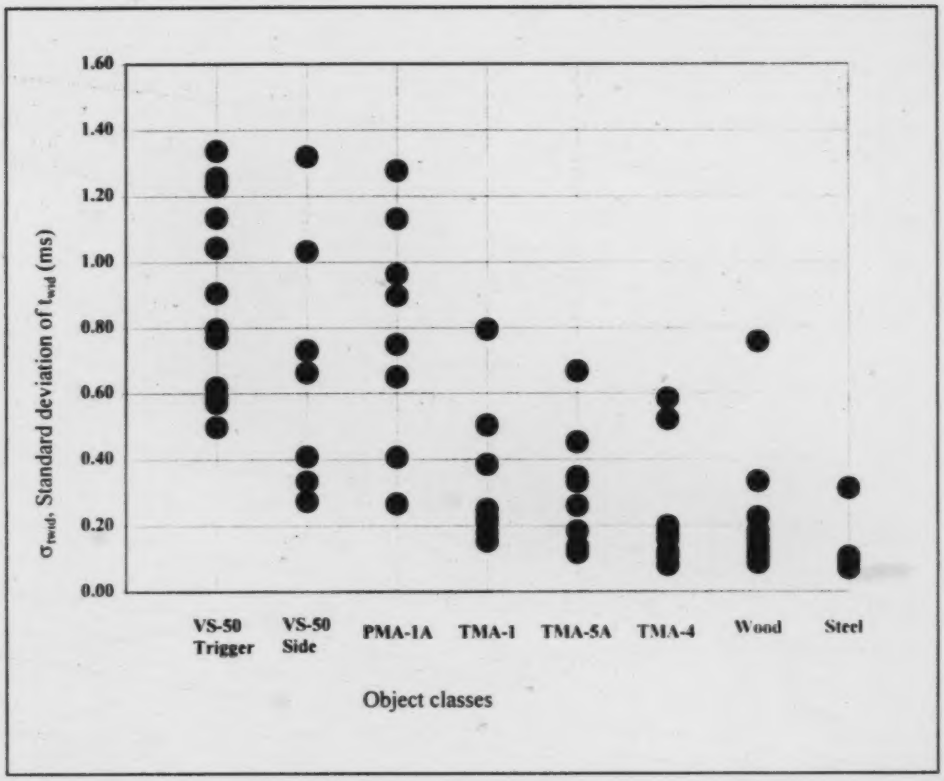

Figure 4.6: The standard deviation of the variable t_{wid} for each object type. Each data point represents the average of ten strikes in succession on a specific region of an object.

CHAPTER 5

ARTIFICIAL NEURAL NETWORKS AND PATTERN RECOGNITION

In order to correctly classify an object, it is necessary to discover the features of the vibration signal which make it different. To assist in this process, a form of artificial neural network (ANN) known as an Adaptive Logic Network (ALN) was employed. An introduction to ANNs will be discussed along with the specific features of the ALN type of network.

ANNs are computer algorithms derived from the model of neural synapses of the human brain.[Hagan, 1-8] The essential concept is to identify a certain output based on a series of inputs. In order for learning to occur, the synapses need to be exposed to inputs multiple times until the proper output is learned. Learning (or training) is performed by reinforcing certain synaptic pathways and making other pathways weaker. The decision for reinforcing or weakening is based on a prescribed learning rule. The type of learning rule used identifies the type of ANN being used.

5.1 Feed-Forward Networks with Supervised Learning

Artificial Neural Networks such as the ALN network use a type of network called a feed-forward network with supervised learning. The feed-forward network uses a learning process to match a set of known input features to a known output state by

a process of trial and error. The input features form what is called a training set. Through training, the network learns to match the inputs to the correct outputs. The best training result for correct classification is when small changes in the input features cause only small changes in the output of the network. Learning occurs after multiple recursive attempts to obtain the correct output as described by the features of the training set. A process may be defined as supervised learning if, as in the case of pattern recognition, the output is known during the training process. The ANN software attempts to minimize the error between the solution (the correct object classification) and the network output (the object classification learned by the network). This is typically an iterative process which can be very slow for large training sets of data.

Also, a solution is often not guaranteed. Usually the number of necessary features to provide a solution is not known. If too few are used, the case may arise that identical input feature values represent different output values. In this case, no solution can ever be found. If too many features are chosen, the speed of learning may be too slow for many practical applications.

5.1.1 An Illustrative Example of Object Classification Using Input Features

The following is an example of how an ANN learns to associate an object type to a set of input features. Consider two objects, a balloon and a baseball. The features chosen must adequately define differences between the objects which makes each object distinct. For instance, defining a feature to describe the roundness or curvature of the object would not be very successful since both objects are roughly round. The balloon and the baseball will respond quite differently to the application of an outside force, however. One could hit the object with a baseball bat and measure the distance the object travels. The measured feature would then be the distance, and it could have ranges from 0 to 300 feet. Obviously the baseball (on average) will have values significantly larger than the balloon. The exact distance the object travels will not

be the same from hit to hit. Parameters such as the person hitting and wind will influence the exact results, but clearly the baseball will travel much farther than the balloon. Another parameter that could be chosen is the colour of the object. There may be some instances where the balloon and the baseball are the same colour, but the balloon can be many different colours while the typical baseball is white.

An ANN could be trained to distinguish the difference between balloons and baseballs using the three features, roundness, distance and colour described previously. In order to apply ANN software to the task of classification, physical features of the objects must be reduced into numeric quantities. For the roundness feature, imaging software may be used that captures an image and defines the curvature of the surface. A value of 0 would be assigned to an object such as a box, and 1 would be assigned a perfect sphere. Thus the feature would have values ranging from 0 to 1. The distance variable would have values ranging from 0 to 300 as stated before. The range of colour could be reduced to a table of assigned values. For instance, one could limit the colours to 16 (white = 1, red = 2, blue = 3, etc.). The range for the colour variable would be from 1 to 16. The choices of the order of colours and the values assigned to them is arbitrary.

Numeric values could be assigned to the features once a series of experiments were performed on each object. The only remaining numeric quantization is for the objects themselves. One could assign the value of 0 to a balloon and 100 to a baseball. The ANN would learn a function that has an output ranging from 0 to 100. During supervised learning, the known network output would be 0 for a set of balloon features and 100 for a set of baseball features. For example, consider the following table of values which could represent the features and objects:

Table 5.1 : Example of features used to train an ANN

Roundness	Distance	Colour	Object
0.95	3.5	3	0
0.98	210	1	100

During the learning phase, an ANN associates the three features of roundness, distance and colour to the output class. In the very beginning of learning, the associations are randomly initialized. The ANN begins to learn an appropriate association through an iterative process. At the end of each iteration, the output of the ANN is compared with the known object class number. The network typically responds by minimizing the error between the known object class number and the network output. As the iterations progress, the error between the output and the known class number is reduced.

Because the input features contain some amount of noise and variability, there exists the potential for the network to learn the noise in the data. In this circumstance, the network is said to be overtrained.[Armstrong, 67] An overtrained network may have an overall network error that is very low, but will perform poorly when new validation data is presented to the network. For example, an ANN may learn that baseballs must have a distance variable that equals 210 exactly. When presented with new data that has a distance value of 190, the network may wrongly classify the object as a balloon. The best network is one that learns the underlying function without memorizing the noise in the data set. Clearly this is a difficult and somewhat arbitrary concept to apply to a data set which contains an unknown amount of noise.

Additional objects could be assessed by the ANN to determine if the object is more like the balloon, or more like the baseball. If the object were a grapefruit, the network may have difficulty deciding which class to which this new object belongs. The distance variable may be closer to the baseball in range, but the colour variable

would more closely resemble the balloon. It may turn out that two networks trained from the same data set will produce different classifications of this new variable. A new function may be required that is trained on data collected from this new object.

5.2 Adaptive Logic Network (ALN)

There are many types of Artificial Neural Networks which are applicable for pattern recognition. These networks associate input features of the original signal to a known output state by using a specified learning rule. It is this learning rule that makes each type of network unique.

5.2.1 The ALN Function

The Adaptive Logic Network creates a function or algebraic equation, the output of which is a number which is associated with an object. Continuing the example of the balloon and the baseball objects, a balloon may be assigned an output, y, of 0 while a baseball may be assigned an output of 100. Each of the input features such as the roundness, distance and colour (x_1, x_2, x_3) is multiplied by a constant or weight (w_1, w_2, w_3) as in the following example equation:

$$w_0 + w_1x_1 + w_2x_2 + w_3x_3 = y$$

where $y =$ the output of the network function

$w_i =$ network weights

$x_i =$ numeric input features

More complex ALN networks implement several of these equations to describe the whole function. Each individual equation may be called a linear piece of the total function. In this way, functions with curvature can be approximated with piecewise linear segments. Figure 5.1 shows the scatter plot of the feature t_{wid} and the object associated with it. Each data point represents the average of ten strikes in succession on a specific region of an object. Three lines are shown to represent the function that

linear piece is used to provide the output y for the network. As training progresses, the ALN software decides which line will be adjusted to reduce the error of the network output when compared with the actual object identification number.

5.2.2 ALN Learning

The weights, w_i, of the network are randomly set at the beginning of the learning procedure. During learning, the weights are either strengthened or weakened to match the output, y, with the known output. This process uses the ALN learning rule of piecewise linear regression to minimize the error between the output of the network and the known result. If there is only a single input feature x_1, the error minimization procedure is analogous to linear regression.

The decision of how to choose the linear piece's range and how many pieces to use is not arbitrary. The ALN decides where the boundaries of the pieces belong by adjusting the slopes of the line segments to minimize the overall error in the output of the function. As mentioned earlier, only one linear piece is active over a given range of the input features. The weights of this linear piece are adjusted during error minimization.

The specific type of function for classification of objects is not known before training the ALN network. To ensure that enough linear pieces are used to cover the input feature space properly, a large network is recommended. The network should contain multiple layers of linear pieces. This is called a *ragged tree*, and is used when the shape of the function in question is not known.[Armstrong, 45]

Note that the weights w_i correspond to the partial derivative of the function with respect to that variable. Limits can be set on the partial derivative to apply real world knowledge about a particular variable. By limiting the partial derivatives the user is able to directly apply knowledge of how the input features should change when the output changes. For the identification of the signals in this study, several relationships between the output and the signal pattern were determined. For instance, when the

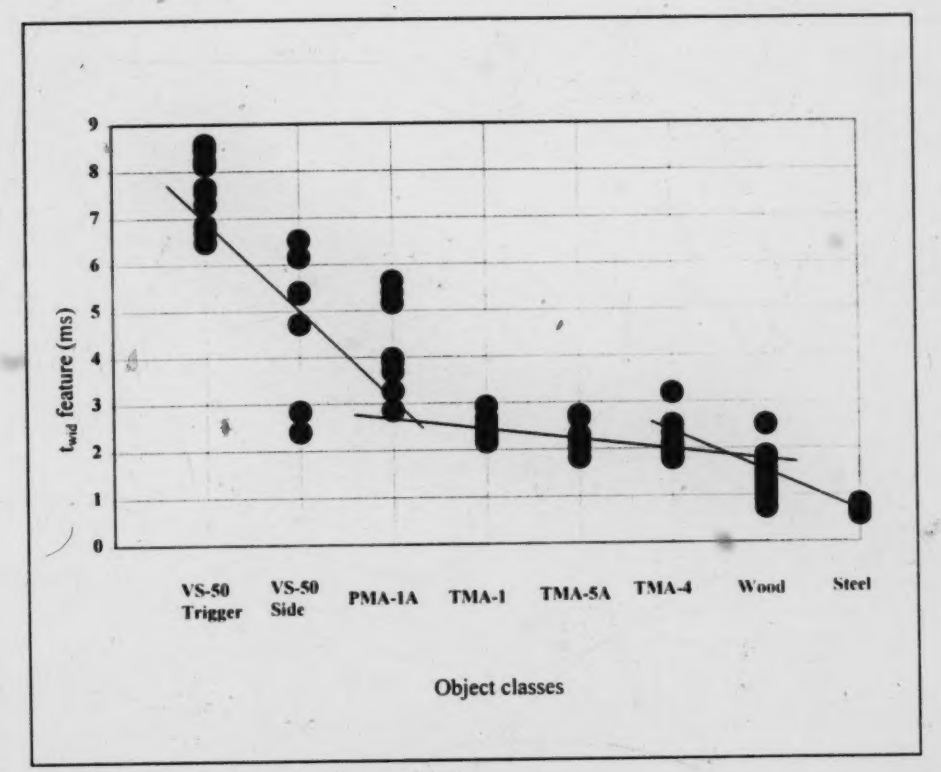

Figure 5.1: ALN classification using the variable t_{wid}. Several lines are used to approximate curvature of a function. The more lines that are used, the better the approximation. Each data point represents the average of ten strikes in succession on a specific region of an object.

prodder struck a stiffer object, the width of the pulse was found to be narrower. Thus the feature t_{wid}, stiffer objects should have smaller t_{wid} values than less stiff objects. By lining up the object classification numbers from less stiff to stiffest (1 being least stiff, 100 being most stiff), we know that this variable will decrease as the output (the classification number) increases. Also, the peak frequency band location should increase when the spring stiffness of the object increases. This information was applied directly into the ALN. Thus, during the training phase, the network learned the classification of the objects along a more specific (rather than general) approach.

5.3 ALN Training

In order to develop a classification function, a function must be trained with data sets known to represent the correct output. This data set is known as the training set. Some of the experimental data was reserved in a test set which was used to evaluate the learned function. The success of this method lies in having enough points that sufficiently describe the objects in question. Once the appropriate function has been found, the evaluation of the function is performed very rapidly. For any given set of input variables, the ALN function only uses one specific line segment to provide the function output. Comparisons are made extremely quickly by the network to find this line segment. This allows classification of signals to take place in near real time.

5.3.1 Object Classification Using an ALN Network

Objects were assigned class identification numbers from 1 to 110 for the purpose of training the network. For instance, PMA-1A was assigned the number 20, TMA-4 was assigned 70. The reason for choosing a specific object number is discussed in the following section on network optimization. The numbers chosen to represent an object were chosen to assist the ALN network in learning the correct result for the input features. The network had to learn a function which associated the input features of each object with the number representing the proper class identification. The network

output, y, should equal the assigned identification number for each object. That is, $y = 20$ is the correct network output for PMA-1A input features. An ideal network would produce a scatter plot where the network output exactly matches the assigned object identification number. Because real networks do not perfectly conform to the training set, there is some imprecision in the network's output for a known object identification number. Table 5.2 shows an ideal network output for exact object classification.

Table 5.2 : Example of an ideal ALN network output.

Object and Class Number	ALN Output
VS-50 Trigger: 1	1
VS-50 Side: 10	10
PMA-1A: 20	20
TMA-1: 40	40
TMA-5A: 60	60
TMA-4: 70	70
Wood: 80	80
Steel: 110	110

5.4 Network Optimization

Several different networks were developed to find the best classification method. The following section describes some of the methods pursued to arrive at the best results when developing the ALN.

5.4.1 Number of strikes with prodder

The number of strikes in succession on a particular region of an object was adjusted from 2, 5 and 10 strikes which were averaged together prior to extracting features. Of

the databases created in this way, the best results came from the 10 strikes averaged together database.

5.4.2 Overtraining the Network

The network overall RMS error was also used as a criterion for a successful network. This value is determined during training as the overall network classification error. If this error is too low, however, the ALN begins to learn the noise in the data rather than a descriptive function for the data. This is not desirable since the network function should not depend on an exact match to the training set data to provide the proper output. Table 5.3 and Table 5.4 display an over-trained network output using training data for the input and the evaluation of this network with test data. The tables show the range of network output values that are determined from the input data. This is also shown graphically in the scatter plots of Figure 5.2 and Figure 5.3. The plots shows the object class against the network output. While the trained network appears to have excellent results in Table 5.3 using the training data, Table 5.4 shows the evaluation of this ALN on the test set is quite poor since several classes of objects overlap.

Overtraining results when the training procedure is continued beyond the point where the network is learning a representative function. This can occur during training when the desired network error is too small. It is a delicate balance to prevent overtraining and still allow the learning to continue long enough to properly learn the classification function. Only through trial and error is this balance established.

Table 5.3 : An overtrained network response to training set data.

Object and Class Number	Range of ALN Output
VS-50 Trigger: 1	1.06 - 1.06
VS-50 Side: 10	9.97 - 9.97
PMA-1A: 20	19.9 - 21.1
TMA-1: 40	39.6 - 40.7
TMA-5A: 60	53.8 - 61.9
TMA-4: 70	66.9 - 75.2
Wood: 80	77.0 - 84.1
Steel: 110	108.0 - 110. 0

Table 5.4 : An overtrained ALN response to the test data set.

Object and Class Number	ALN Output
VS-50 Trigger: 1	5.16 - 24.4
VS-50 Side: 10	28.6 - 45.0
PMA-1A: 20	20.1 - 25.2
TMA-1: 40	29.7 - 43.5
TMA-5A: 60	54.5 - 59.1
TMA-4: 70	66.3 - 75.3
Wood: 80	67.7 - 84.7
Steel: 110	81.3 114.6

5.4.3 Object Numbering and Order

The network will have the most success (lowest RMS error and best classification) if the object classes are ordered in a meaningful way. The stiffness of the object is the

most dominant variable for the objects. Arranging the objects in order of increased stiffness improved the learning and evaluation of the network. By arranging the objects in such an order, the knowledge gained from the theory could be directly incorporated into the network learning. Random arrangement of the object classes produced poor network learning with large overall errors.

Numbering the objects in even spacing from 1 to 8 was found to be less successful than the ordering shown in Table 5.2. The numbering chosen groups some of the objects closer together than others. For example, the VS-50 mine trigger and side and the PMA-1A mine were each separated by 10 points, whereas the steel object is separated from the wood object by 30 points. This separation assists in classification.

5.4.4 Features Attempted and Rejected

Other features were attempted in addition to the 19 time and frequency domain features discussed previously. These included the standard deviation of the frequency band components and the location of the peak frequency component. ALNs were formed with the inclusion of these features in the learning of a network function. It was found that when these features were removed from the learning procedure, the ALN overall error did not change. These particular features did not assist in forming a meaningful function which could classify the objects.

Also attempted were evenly spaced frequency bands. Training was observed to improve once the bands were chosen to emphasize the lower frequency range of the acceleration signals.

5.5 ALN Results

After the ALN networks were trained, they were evaluated using the test set data. The minimum separation between any two object classes was 10 units. An ALN network was determined to be successful if it could classify an object to within 5 units of the actual class identification number. This would mean that no two objects

would ever cross into the same object classification range. For instance, a VS-50 AP mine was assigned the identification number 1.0. The network output (y) should then be 1.0. Since the network is not perfect, an output of 1.0 to 5.0 may result.

After extensive experiments with different forms of ALNs, no ALNs trained could distinguish all objects independently from the other objects to within the 5 point criterion. All the trained networks classified at least one object as the wrong object.

The ALN networks frequently confused the object classes for TMA-1 and TMA-5A. There was also some misclassification of AT mines as being wood objects. The reason for this misclassification stems from the fact that the original vibration data for these types of objects are very similar. As a result, the network attempts (and fails) to distinguish very similar input features with distinctly different output values. Where the vibration data is not as similar, the network has more success. Significantly, there was no misclassification of any mines as being steel objects.

5.5.1 Results of the Best ALN Classification

The results of the best ALN network trained can be found in Table 5.5. One important feature of this network is that no land mines were ever mistaken for the steel object. There is a clear separation between the object classes with limited overlap only between the AT mines TMA-4 and the TMA-5A. Table 5.5 shows the network outputs representing TMA-1 and TMA-5A overlap. This is also shown in the scatterplot of Figure 5.4. For the TMA-1 and TMA-5A objects, the network has difficulty correctly associating the input features with different objects. The input features for these two objects are very similar which may explain the error in the network.

Table 5.5 : Results of the best ALN network evaluated on the test data sets.

Object and Class Number	Range of ALN Output
VS-50 Trigger: 1	1.07 - 3.44
VS-50 Side: 10	6.88 - 14.5
PMA-1A: 20	15.2 - 24.4
TMA-1: 40	28.2 - 53.2
TMA-5A: 60	27.9 - 60.6
TMA-4: 70	38.5 - 71.3
Wood: 80	80.9 – 87.8
Steel: 110	101.1 - 110.0

5.6 Conclusions of ALN Object Classification

Many attempts were made to create an ALN that could correctly classify each object into its appropriate category. The best ALN results were from ALNs trained on feature databases were 10 signals were averaged together. Also, the objects needed to be arranged into an order which promoted the best ALN training. Typically this meant arranging them from the least to the most stiff objects.

The best classification of objects could correctly identify most of the objects independently of the others. The TMA-1 and the TMA-5A AT mine could not be uniquely distinguished. This is not considered to be a significant concern since the joint class containing both mines could be formed. By doing this, the joint class is identified independently of the other objects tested.

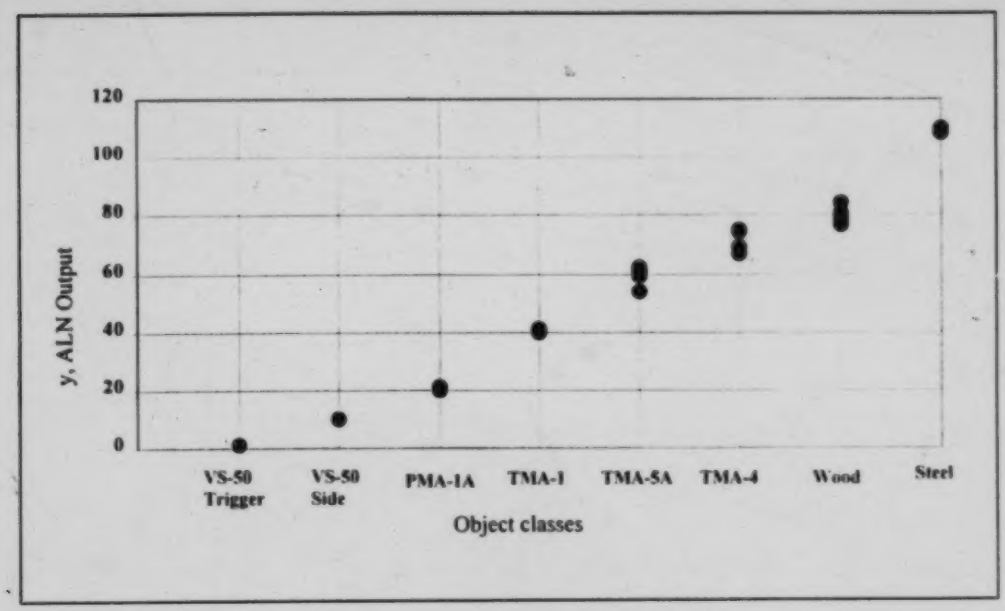

Figure 5.2: A scatter plot of an overtrained ALN output using training data as the input.

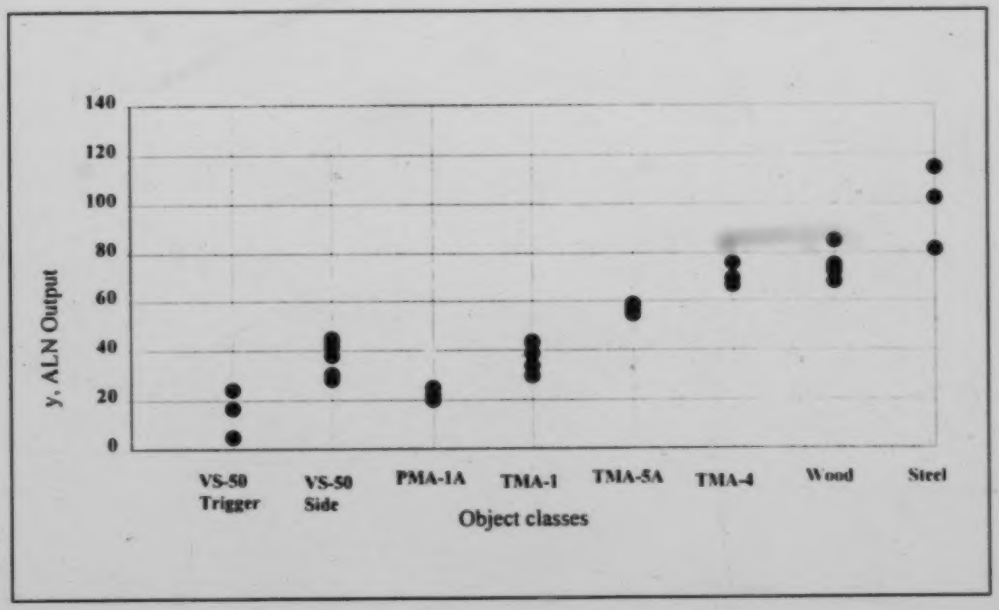

Figure 5.3: A scatter plot of an overtrained ALN output using test data as the input.

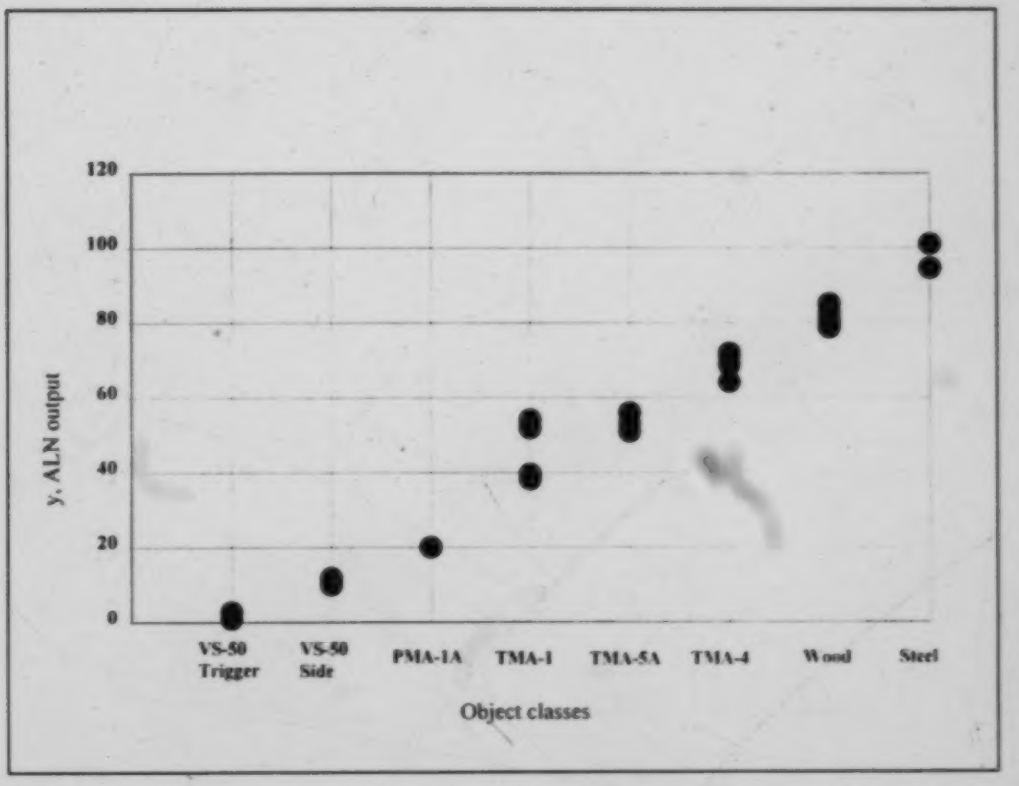

Figure 5.4: ALN output vs. actual using the training database to evaluate the ALN.

Chapter 6

Conclusions and Future Work

There is an absence of safe, accurate and cost effective land mine detection technologies currently available. The preceding chapters describe a technique for the safe and accurate detection of land mines based on the hand prodding technique. Automating this process will provide increased safety and decrease the amount of time required to locate each hidden land mine. The reduction of false alarms and faster detection rates are the goals of this current work.

Ideally, an automated device will work with the capacity of many field personnel with hand held prodders methodically striking the ground. Unlike non-contacting devices, physically prodding the ground will ensure that every square inch of land covered by the system have been passed over and tested. In this case, if the device should fail to detect the presence of a mine or should the mine be accidentally detonated, the automated prodder will be damaged. Human operators will not be in direct contact with the exploding land mines.

6.1 Conclusions of Current Work

Automated prodder detection technology has been proven to work successfully in the identification of hidden objects. Predictions using theoretical models of the prodder and object system provided quantifiable features intrinsic to the type of object. The stiffness of the object in question plays a role in classification, but is not the only

property of the mine which determines the vibration signal observed in the prodder and object system.

The prototype used to evaluate the automated prodder struck buried objects with approximately the same velocity. It was found that ten strikes taken on the same spot of the hidden object and averaged together provided the best object classification.

The acceleration data from the prodder's contact with the objects was reduced into a series of features in the time and frequency domains. These features were used by ALN artificial neural network software to create and evaluate learned functions which identify the hidden object. The ALN function learned using this experimental data was shown to successfully identify certain classes of hidden objects as distinct.

Artificial neural networks such as ALN's are susceptible to overtraining. Overtraining results when training progresses too long and the noise in the input database is memorized by the ALN. As a result, new data is poorly classified. Correct training will prevent the overtraining of the ALN while allowing the reduction of the overall network error to the lowest possible value. This balance is often difficult to achieve and several attempts must be made before the best ALN function can be found.

The ALN that had the best evaluated results showed that no land mines were ever classified steel debris. This means that false alarms due to contact with rocks and steel debris will be nearly eliminated. While objects such as steel and the AP mine VS-50 were easily classified, the ALN function had difficulty separating objects with similar vibration characteristics. Similar object stiffnesses have similar object feature values. This makes classification of similar objects difficult. For instance, the AT mines TMA-1 and the TMA-5A could not be distinguished during the evaluation phase of classification. This is likely due to the fact that these two mines have very similar stiffnesses. On the other hand, the dissimilar stiffnesses of the AP mine VS-50 and the steel block made separating these objects into separate classes successful.

6.2 Future Research

A single prodder has been proven to successfully identify specific classes of hidden objects in the lab. To make the device more useful, field trials will be necessary. Different soil environments including soil types, gravel, moisture and vegetation need to be investigated. Field test should consider uneven terrain and excessive vegetation in the design of the prodder deployment. In order to accomplish this, some type of portable device will be needed. Once this has been completed, an array of prodders could be designed and tested by mounting them on a truck, all terrain vehicle or armoured car. If this proved useful and live tests were considered appropriate, a remotely controlled all terrain vehicle would remove the need for a human operator close to the mine field. Also, the armoured car could provide a shield from any accidental explosion from land mines.

The number of prodders in the array is flexible and can be adapted to suit the requirements of a specific environment. It is conceivable that three, ten or dozens of prodders could be joined together to detect land mines in a particular area. As the number of prodders grows, the computing power required to control and evaluate the acceleration data recorded must be considered.

This developed technology is not meant to be used as a stand alone detection method, but rather to be used in conjunction with other mine detection devices as outlined in Chapter 1. Integration with other detection devices will improve the detection success rate to the near 100% required.[Hanshaw, 249-256. Garriott, 259-268. Chaudhuri, 187-204.] For instance, ground penetrating radar can be used to first identify areas of land mine fields. The prodders could sweep the area in question for land mine objects. Once a potential mine object is discovered, explosive detectors and bio-sniffers can confirm the identity of the mine by locating concentrations of explosives.

The ALN software used to develop the identification function can be used to adapt to new types of objects as they are encountered in the field. This will require that the

vibration data is stored in the field computer and that the types of objects are known. New training and evaluation databases can be created to form new identification functions that are adapted to a particular region. Currently the signal processing to accomplish this is done using Matlab software. This could be rewritten using C++ or a similar programming language to create faster feature reduction.

The ALN software was chosen for its ease of use and local support. There are several artificial neural network types which are applicable for object classification applications. Future work could determine which type of artificial neural network was the most appropriate for the types of input features used in this study.

The features chosen to represent each object have been shown to work in the lab environment. It should be confirmed that these features are applicable for generic conditions found in the field. It should also be discovered if the ALN trained in one environment can be used to detect mines found in another environment. The ALN may need to be retrained using specific tests performed in each type of soil condition.

REFERENCES

Armstrong, William W. and Monroe M. Thomas. *Atree 3.0 User's Guide.* Dendronic Decisions Ltd., 1996.

Chaudhuri, Sam, Alan Crandall, and Denis Reidy. "Multisensor Data Fusion for Mine Detection". *SPIE.* Vol. 1306 pp. 187-204 (1990)

Craib, J.A. "Survey of Mine Clearance Technology." Technical Report. The United Nations University and The United Nations Department of Humanitarian Affairs. September 1994.

Focsaneanu, G. "Mechanical Clearance: A Long Overdue Essential Solution to the World's Mine Problem" in *SusDem '97: International Workshop on Sustainable Humanitarian Demining.* Zagreb, Sept. 29-Oct. 1, 1997.

Garriott, Ray, David Lang, James Nilles et al. "A Multisensor System for Mine Detection." *SPIE.* Vol. 2765 pp. 259-268 (1996)

Hagan, Martin T., Howard B. Demuth, and Mark Beale. *Neural Network Design.* Boston, Mass.: PWS Publishing : International Thomson Publishing, 1995.

Hanshaw, Terilee. "Multi-Sensor Application for Mines and Mine-Like Target Detection in the Operational Environment." *SPIE.* Vol. 2765 pp. 249-256 (1996)

Konrad, J.M. "Frost heave mechanics." Ph.D. Thesis, Department of Civil Engineering, University of Alberta, Edmonton, 1980.

LabVIEW Data Acquisition Basics Manual. National Instruments Corporation, January 1996 ed.

Lukas, D. and W. Schulte. "Periotest: A Dynamic Procedure for the Diagnosis of the Human Periodontium." *Clinical Physical Physiological Measurements.* Vol. 11 No.1 pp. 65-75 (1990)

Lynn, Paul A. and Wolfgang Fuerst. *Introductory Digital Signal Processing with Computer Applications.* Rev. ed. Chichester, Eng.: John Wiley and Sons, 1994.

McFee, John, Yogadish Das, and Al Carruthers, et al. "CRAD Countermine R & D Study – Final Report". No. 173. Department of National Defense, Canada. Defense Research Establishment Suffield, 1994.

Rao, Singiresu S. *Mechanical Vibrations.* Reading, Mass.: Addison-Wesley, 1986.

Slavin, S.E. and G.T. Beswick. "Instrumented Izod Impact Testing." *Journal of Applied Polymer Science.* Vol. 49 pp. 1065-1070 (1993)

Thomson, William T. *Theory of Vibration with Applications.* 3rd ed. Eaglewood Cliffs, NJ: Prentice Hall, 1988.

United States. Office of International Security Operations. "Hidden Killers: The Global Problem With Uncleared Landmines – A Report on International Demining." United States Department of State, Political-Military Affairs Bureau, 1993.

Appendix A

Object Properties

The stiffnesses in the following table were used in the modeling of the prodder and object impulse system found in Chapter 2. The stiffness of the objects was determined using an INSTRON testing instrument. The $\frac{1}{4}$ inch steel prodder was attached to the INSTRON test unit and was then moved at a constant displacement rate into the various objects. The force required was simultaneously monitored. The stiffness of each object was obtained by dividing the force by the distance the prodder pushed into the object. The stiffness of the VS-50 AP mine was found for both the softer trigger pad located in the center of the mine, and on the hard plastic side of the mine. All objects were observed to elastically deform with the exception of the wood block. As the prodder was forced onto the wood block, a hole was formed. Subsequent stiffness tests on the same hole showed that the stiffness increased to about 7 times the original stiffness. The steel block was not tested with the INSTRON. It is assumed that the steel block is much stiffer than any of the other objects tested.

Note that the construction of the PMA-1A AP mine consisted of a box with a lid. The initial applied force of the INSTRON machine caused the lid to close and compress. After the slack was taken out of the system, the plastic lid was compressed. A consistent stiffness value for the lower load region was not observed. The stiffness value shown in Table A.1 was calculated for the plastic lid compression.

Table A.1: Physical properties of the objects used during testing.

Object	Diameter (mm)	Height (mm)	Width (mm)	Length (mm)	Mass (kg)	Stiffness (kN/m)
VS-50	90	45	NA	NA	0.185	5.60 (trigger pad) 237 (plastic)
PMA-1A	NA	33	68	143	0.400	1180
TMA-1	315	100	NA	NA	6.50	94.2
TMA-5A	NA	113	275	304	6.50	55.2
TMA-4	285	63	NA	NA	6.30	34.2
Pine Wood Block	NA	51	76	152	0.500	57.1 (soft) 416 (hard)
Steel	NA	13	51	76	2.00	NA
Soil	Using 10" disk	NA	NA	NA	NA	26.1

Appendix B

Theoretical Models for the Prodder and Object Impulse System

B.1 Two degree of freedom model eigenvalues

This more detailed model introduces a second natural frequency and natural mode of vibration to the system. The mathematical term for mode is an eigenvector, while eigenvalues correspond to the natural frequencies. An eigenvector is a displacement configuration which shows how the masses are moving in relation to one another. Each eigenvector has a corresponding eigenvalue. For a system with 2 degrees of freedom, there will be 2 eigenvalues each with its own eigenvector. If the system is given an initial excitation in the form of an impulse, the system will vibrate at the frequencies of the eigenvalues. The shape and amplitude of the vibration is described by the eigenvectors. Eigenvectors are used to define the relative contributions each of the eigenvalues have on influencing the shape of vibration.

Analysis of the force balance on each of the masses in this system provide the equations of motion used to determine the eigenvalues and eigenvectors. In matrix form, the equations are as follows:

$$[m]\{\ddot{x}\} + [k]\{x\} = \{0\}$$

The mass matrix is defined for this system as:

$$[m] = \begin{bmatrix} m_p & 0 \\ 0 & m_{obj} \end{bmatrix}$$

and the stiffness matrix is:

$$[k] = \begin{bmatrix} k_{obj} & -k_{obj} \\ -k_{obj} & k_{obj} + k_{soil} \end{bmatrix}$$

The characteristic equation for this system of equations is:

$$\omega^4 m_p m_{obj} + (-k_{obj} m_{obj} - m_p k_{obj} - m_p k_{soil})\,\omega^2 + k_{obj} k_{soil}$$

It has has the following eigenvalues:

$$\omega^2 = \frac{k_{obj} m_{obj} + m_p k_{obj} + m_p k_{soil} \pm \sqrt{\left((k_{obj} m_p + k_{soil} m_p + k_{obj} m_{obj})^2 - 4 m_p m_{obj} k_{obj} k_{soil}\right)}}{2 m_p m_{obj}}$$

To find the system's eigenvectors, we can assume a solution to the differential equation in the form of:

$$x_1 = A_1 e^{i\omega t}, \quad x_2 = A_2 e^{i\omega t}$$

Substituting these into the original equations of motion gives:

$$e^{i\omega t} \begin{bmatrix} m_p & 0 \\ 0 & m_{obj} \end{bmatrix} \begin{Bmatrix} -A_1\omega^2 \\ -A_2\omega^2 \end{Bmatrix} + \begin{bmatrix} k_{obj} & -k_{obj} \\ -k_{obj} & k_{obj} + k_{soil} \end{bmatrix} \begin{Bmatrix} A_1 \\ A_2 \end{Bmatrix} e^{i\omega t} = \{0\}$$

Solving this equation for A_1 and A_2, the following ratio is obtained:

$$\frac{A_1}{A_2} = \frac{k_{obj} + k_{soil} - m_{obj}\omega^2}{k_{obj}} \leftrightarrow \omega = \text{the corresponding eigenvalue.}$$

The eigenvector is the ratio of amplitudes of the two vibrating objects. This eigenvector depends on the eigenvalue. If the ω is large, then the ratio becomes:

$$\frac{A_1}{A_2} \simeq \frac{-m_{obj}\omega^2}{k_{obj}}$$

For large ω, the soil compression does not influence the vibration amplitude ratio significantly. For small values of ω, the eigenvector becomes:

$$\frac{A_1}{A_2} \simeq \frac{k_{obj} + k_{soil}}{k_{obj}}$$

At small ω, the mass of the object does not influence the vibration ratio. If the soil spring constant k_{soil} is small compared to the object, this ratio becomes 1. This means that the object and the prodder would be moving in unison.

B.2 Continuous System

This section will discuss the possibility of a compressible prodder. It will be shown that the lowest natural frequency of the prodder depends on its length.

The prodder can be modeled as a homogeneous, isotropic elastic thin bar which has an infinite number of DOF. Longitudinal vibrations of the bar can be studied by performing a force balance on an infinitesimal longitudinal section (shown in Figure 8). Such analysis is available in several textbooks.[Timoshenko, Thompson] The natural frequencies are found to depend on the boundary conditions of the bar. For this case, the prodder can be modeled as free on one end and fixed on the other. This leads to the following natural frequencies [Timoshenko, 302]:

$$\omega = \frac{(2n+1)\,\pi}{2L}\sqrt{\frac{E}{\rho}}$$

Where:

n = $0, 1, 2, \ldots$

L = Bar Length

E = Young's Modulus

ρ = Density

An impulse excitation force in this system will cause all modes to vibrate simultaneously. These frequencies occur regardless of the object struck provided the excitation and boundary conditions remain the same. The lowest frequency occurs at:

$$\omega_1 = \frac{\pi}{2L}\sqrt{\frac{E}{\rho}}$$

This is the lowest frequency vibration mode of the prodder. All other modes occur at frequencies above this value. For the prodder used in these tests (a stainless steel cylinder 0.320 m in length), $\omega_1 = 24.6 \times 10^3$ rad/s. or 3.9 kHz. The prodder's vibration should only be noticed at frequencies at or above this value. Thus it should be safe to assume that the prodder can be modeled as a rigid body for frequencies below ω_1.

APPENDIX C

SOFTWARE PROGRAMS USED TO IDENTIFY OBJECT FEATURES

The following sections are computer programs written in LabVIEW and Matlab programming languages. Included here are programs which remove noise from the raw acceleration data, average the signals, and determine the features of the time and frequency domain used in object classification.

C.1 Averaging the acceleration signals.

```
function [y,twid,stw,Awid,sAw,peak,speak] = avgpeak3(x,nsignal)

% x = raw data signals; not lined up
%     1500:nsignal size
% nsignal = number of signals of x we want to average
%    (typically 5, 10 or 20)
% m = value of x minimums (peak)
% n = position of x peak

% y = average of these 'nsignal's
% twid = peak width
% stw = standard deviation of twidth
% Awid = sum of peak amplitudes (normalized )
% sAw = standard deviation of Awidth
% peak = average of the peaks in samples
% speak = STD of peaks

[q,w] = size(x);

x(6000,w) = 0;

[m,n] = min(x);
peak = mean(m);  %peak found
speak = std(m);

nmin = min(n);
```

```
prescan = 40;
if nmin < prescan
   prescan = nmin-1
end

nb = 750-prescan;
init = 0.08; %picked after extensive trial and error

for i = 1:nsignal;
   a = n(i);
   b = ones(1,nb-1).*init;
   c = x( (a-prescan):6000, i)./(-m(i));
   nd = (a-nb-prescan);
   if nd <0
      c = x((a-prescan):(6000+nd),i)./(-m(i));
   end
   d = ones(1, nd).*init;
   xn(i,:) = [ b, c', d];

   adone = 0;
   bdone = 0;
   sum = m(i);
   j = 0;
   counta = 0;
   countb = 0;
   while (~adone|~bdone)
      j = j + 1;

      threshold = -0.1;  %threshold arbitrary

      if xn(i,nb+prescan-j) <= threshold    % width before peak
         sum = sum + xn(i, nb+prescan-j);
         counta = counta + 1;
      else
         adone = 1;
      end
      if xn(i,nb+prescan+j) <= threshold   % width after peak
         sum = sum + xn(i, nb+prescan+j);
         countb = countb + 1;
      else
         bdone = 1;
      end
   end
   twidth(i) = counta + countb;  % width of peak
   Awidth(i) = sum/m(i);         % peak width area
end

% xn contains all the lined up raw input signals
yn = mean(xn);
y = -yn;
twid = mean(twidth);
Awid = mean(Awidth);
stw = std(twidth);
sAw = std(Awidth);
```

C.2 Determination and storage of time and frequency domain features.

```
function [x,twid,stw,Awid,sAw,B,fpeak] = featurefile5(object,nfiles)

% Takes in raw datafile, nx6000 matrix
% Sends out features of N averaged signals
%     --first average, then get features
%     --Saves in file
%
% object = signal file name
% x = object.dat loaded file
% n = 6000 --length of signal (~ sec of data)
% m = # of runs/signals in datafile
% nfiles = # want to average together
% N = # of groups of nfiles available in file
%
% Calls Matlab file: avgpeak3.m

file = ['c:\david\thesis\data\objects\',object,'.dat'] Load raw data
eval('load(file);');
vector = ['x = ',object,''';']
eval(vector);

[n,m] = size(x);
N = fix(m/nfiles)
x = x./5.44e-3;

for i = 1: N

   % Get features from time domain

   y = x(:,((i-1)*nfiles+1):(i*nfiles));%subset of the object file

   [yavg(i,:),twid(i),stw(i),Awid(i),sAw(i),peak(i),speak(i)] =
avgpeak3(y,nfiles);

   % Now get frequency domain
   F = (fft(yavg(i,:))./length(yavg(i,:))) *2; % scaled
   F(1) = F(1)/2; %Correct first sample
   P = F.*conj(F) ;  % Power Spectrum

   B(i,1) = mean( P(1:25) );
   B(i,2) = mean( P(26:50) );
   B(i,3) = mean( P(51:75) );
   B(i,4) = mean( P(75:100) );
   B(i,5) = mean( P(101:200) );
   B(i,6) = mean( P(201:300) );
   B(i,7) = mean( P(301:400) );
   B(i,8) = mean( P(401:600) );
   B(i,9) = mean( P(601:1000) );
   B(i,10) = mean( P(1001:1500) );
   B(i,11) = mean( P(1501:2000) );
   B(i,12) = mean( P(2001:3000) );
```

```
   fpeak(i) = max(P);

end

x = yavg'; % N averaged signal groups --x(6000:N)

% Now save these features in a feature vector.
feature = zeros(N,19);
for i = 1: N
      feature(i,:) = [twid(i),stw(i), Awid(i),sAw(i), peak(i),speak(i),
B(i,:), fpeak(i)];
end
```

APPENDIX D

AVERAGED ACCELERATION PLOTS FOR EACH OBJECT

The following plots are the acceleration signals obtained after averaging ten strikes of the prodder in succession on a particular region of an object.

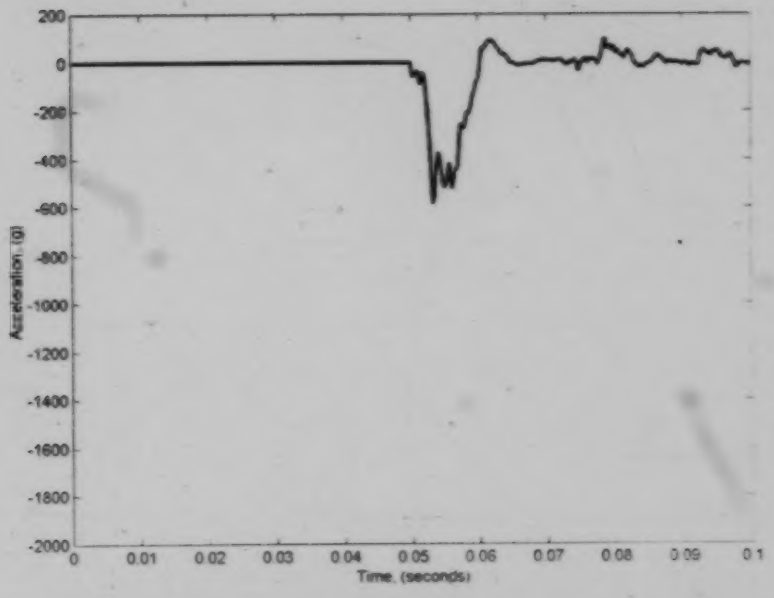

Figure D.1: Time domain averaged plot of AP mine VS-50.

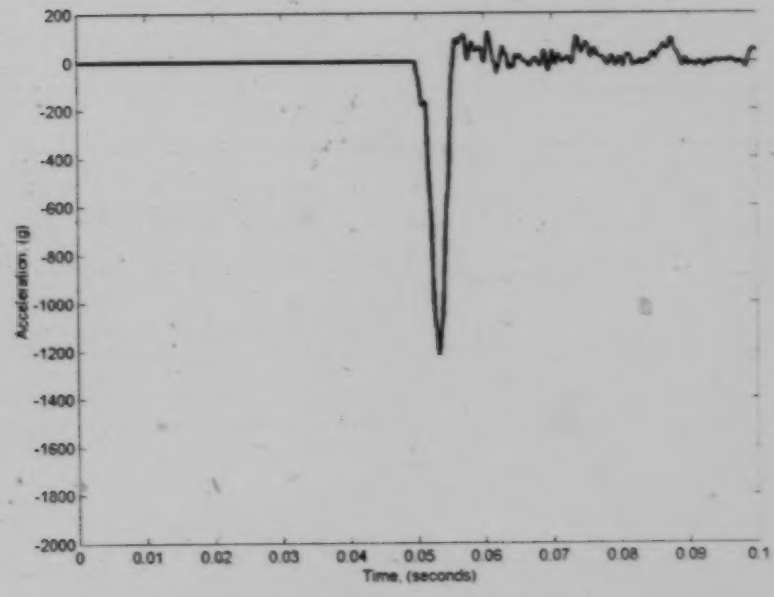

Figure D.2: Time domain averaged plot of AP mine VS-50 side.

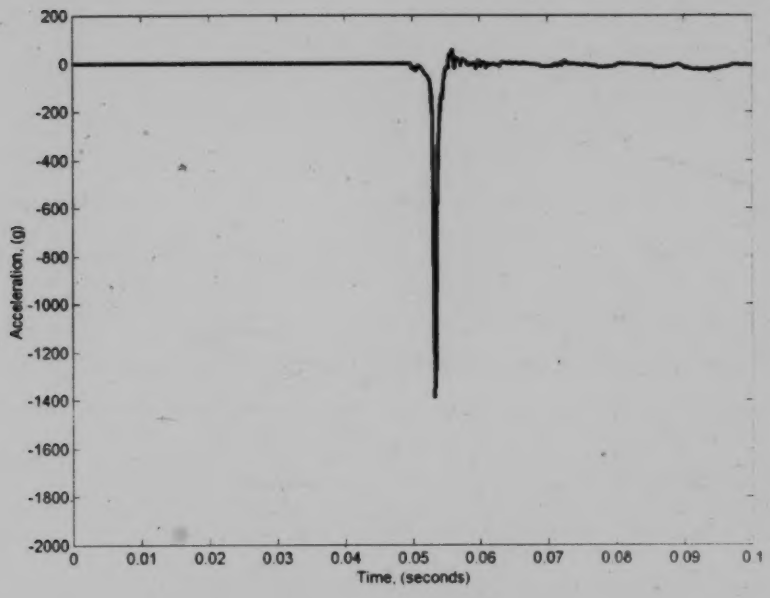

Figure D.3: Time domain averaged plot of AP mine PMA-1A.

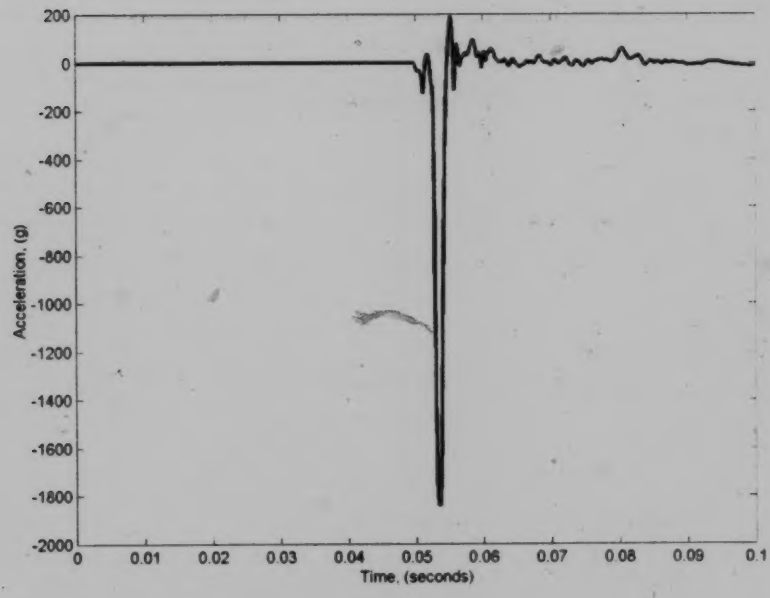

Figure D.4: Time domain averaged plot of AT mine TMA-1.

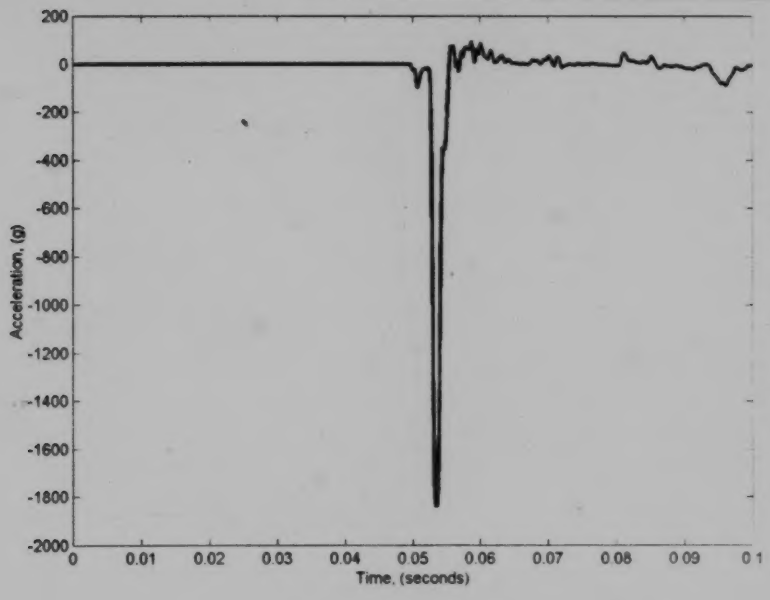

Figure D.5: Time domain averaged plot of AP mine TMA-5A.

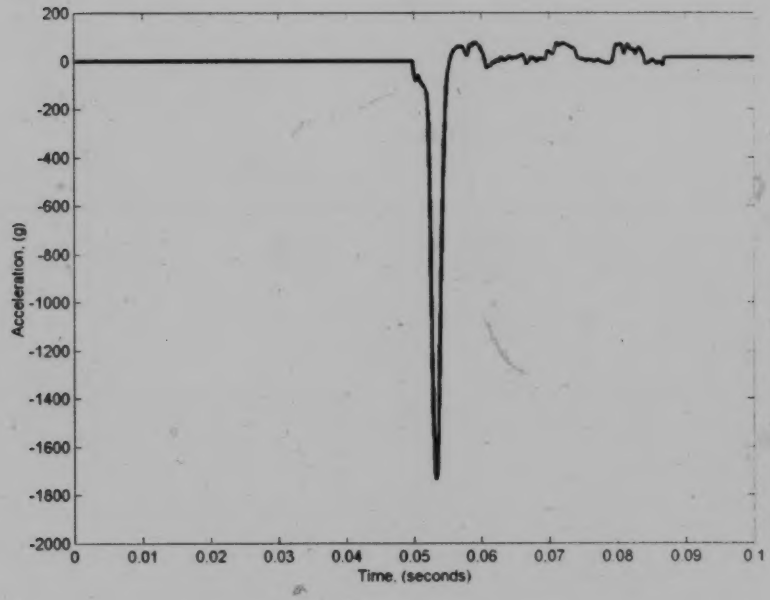

Figure D.6: Time domain averaged plot of AT mine TMA-4.

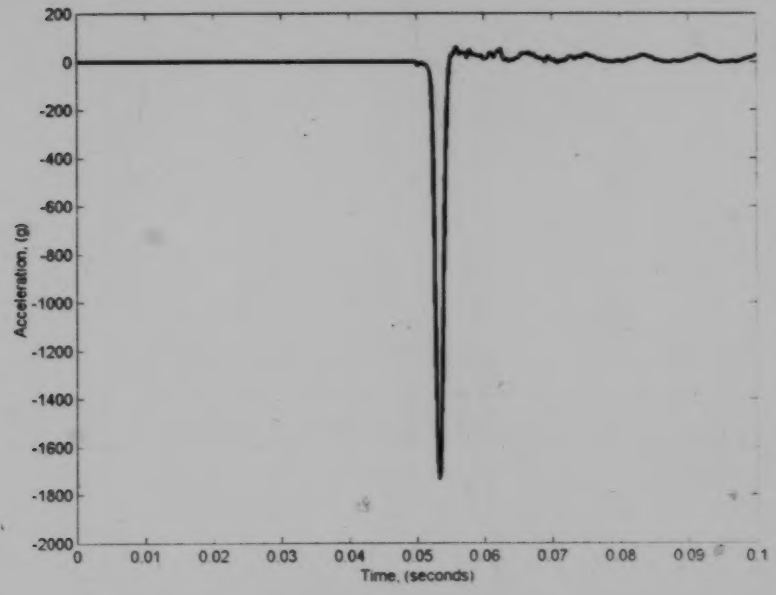

Figure D.7: Time domain averaged plot of wood object.

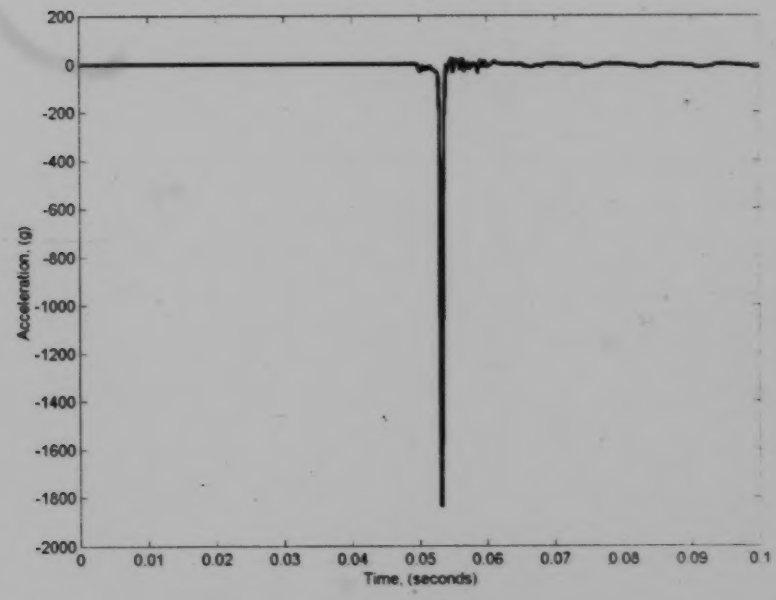

Figure D.8: Time domain averaged plot of steel object.

APPENDIX E

FEATURE VALUES FOR EACH OBJECT

The following tables contain the values of the time and frequency domain features extracted from the raw acceleration signals. Ten strikes of the prodder were made in succession on a particular region of an object. The acceleration signals resulting from contact with the object were averaged together prior to calculating the features. Features were then arranged in a database used to form a neural network function to classify each object.

Table E1: VS-50 AP mine trigger object features

Feature	Values
t_{wid} (ms)	8.47, 8.57, 8.13, 8.15, 8.13, 8.23, 7.55, 7.65, 6.85, 6.68, 7.30, 6.48
σ_{twid} (ms)	0.57, 1.13, 0.77, 0.59, 0.62, 0.50, 1.23, 1.34, 1.26, 1.04, 0.91, 0.80
A (g)	618, 627, 684, 688, 726, 662, 691, 691, 842, 814, 733, 792
σ_A (g)	36, 53, 35, 31, 82, 44, 74, 68, 110, 62, 54, 88
I (g^*s/g_{peak})	0.278, 0.268, 0.235, 0.231, 0.217, 0.242, 0.224, 0.218, 0.172, 0.170, 0.197, 0.174
σ_I (g^*s/g_{peak})	0.024, 0.034, 0.020, 0.015, 0.040, 0.027, 0.040, 0.035, 0.044, 0.024, 0.023, 0.036
F(1-25 Hz)	4.80, 4.56, 4.33, 4.22, 4.12, 4.29, 3.99, 4.02, 3.58, 3.48, 3.75, 3.55
F(26-50 Hz)	2.87, 2.69, 2.38, 2.37, 2.31, 2.49, 2.29, 2.24, 1.86, 1.86, 2.03, 1.86
F(51-75 Hz)	1.87, 1.62, 1.35, 1.52, 1.34, 1.48, 1.43, 1.19, 1.18, 1.32, 1.33, 1.2
F(76-100 Hz)	0.754, 0.581, 0.487, 0.554, 0.554, 0.605, 0.551, 0.554, 0.669, 0.635, 0.642, 0.777
F(101-200 Hz)	0.134, 0.0990, 0.0635, 0.109, 0.125, 0.124, 0.0794, 0.0747, 0.133, 0.157, 0.122, 0.153
F(201-300 Hz) $*10^4$	87.9, 50.0, 31.8, 32.5, 50.7, 38.2, 28.5, 49.0, 65.6, 77.0, 58.5, 71.6
F(301-400 Hz) $*10^4$	145, 200, 234, 228, 173, 149, 149, 261, 220, 159, 203, 179
F(401-600 Hz) $*10^4$	116, 96.3, 73.3, 124, 162, 113, 108, 118, 167, 117, 130, 144
F(601-1000 Hz) $*10^4$	33.4, 38.9, 31.5, 40.2, 36.5, 34.8, 12.4, 12.7, 22.2, 10.8, 8.92, 11.8
F(1001-1500 Hz) $*10^4$	2.93, 3.07, 2.13 , 2.99, 2.53, 2.57, 2.87, 2.55, 1.60, 1.89, 3.37, 1.04
F(1501-2000 Hz) $*10^4$	0.68, 1.21, 0.60, 0.57, 0.53, 1.53, 0.58, 1.15, 0.84, 0.65, 1.30, 0.54
F(2001-3000 Hz) $*10^4$	0.30, 0.32, 0.15, 0.22, 0.24, 0.68, 0.36, 0.36, 0.27, 0.22, 0.47, 0.31
F_{peak}	717, 653, 686, 664, 671, 688, 632, 680, 640, 632, 642, 636

Table E2: VS-50 AP mine side object features

Feature	Values
t_{wid} (ms)	2.85, 3.68, 5.38, 5.63, 3.88, 5.17, 3.27, 3.97
σ_{twid} (ms)	0.267, 0.65, 0.962, 0.748, 1.13, 1.28, 0.897, 0.407
A (g)	1702, 1430, 1059, 930, 1311, 1064, 1570, 1270
σ_A (g)	105, 67, 104, 128, 248, 161, 213, 107
I ($g*s/g_{peak}$)	0.0610, 0.0720, 0.104, 0.123, 0.0797, 0.102, 0.066, 0.081
σ_I ($g*s/g_{peak}$)	0.004, 0.004, 0.015, 0.023, 0.021, 0.021, 0.012, 0.007
F(1-25 Hz)	2.14, 2.22, 2.44, 2.57, 2.26, 2.42, 2.16, 2.31
F(26-50 Hz)	0.625, 0.787, 1.05, 1.24, 0.787, 1.03, 0.669, 0.882
F(51-75 Hz)	0.436, 0.537, 0.787, 0.889, 0.561, 0.713, 0.470, 0.595
F(76-100 Hz)	0.348, 0.392, 0.480, 0.517, 0.405, 0.463, 0.375, 0.463
F(101-200 Hz)	0.264, 0.274, 0.267, 0.248, 0.245, 0.268, 0.242, 0.250
F(201-300 Hz)	0.115, 0.106,0.0906, 0.0804, 0.100, 0.0895, 0.116, 0.110
F(301-400 Hz) $*10^4$	453, 362, 284 ,226, 362, 299, 419, 301
F(401-600 Hz) $*10^4$	75.7, 39.2, 24.4, 29.6, 44.3, 24.2, 67.2, 39.5
F(601-1000 Hz) $*10^4$	2.42, 2.97, 2.05, 2.74, 3.41, 2.86, 1.90, 2.92
F(1001-1500 Hz) $*10^4$	0.61, 0.44, 1.05, 1.16, 1.26, 1.29, 0.47, 1.64
F(1501-2000 Hz) $*10^4$	0.272, 0.285, 0.534, 0.659, 0.500, 0.476, 0.308, 0.568
F(2001-3000 Hz) $*10^4$	0.199, 0.151, 0.375, 0.274, 0.345, 0.261, 0.168, 0.334
F_{peak}	540, 520, 494, 465, 515, 502, 529, 506

Table E3: PMA-1A AP mine object features

Feature	Values
t_{wid} (ms)	2.25, 2.42, 2.67, 2.30, 2.33, 2.27, 2.17, 2.23, 2.55, 2.92
σ_{twid} (ms)	0.18, 0.21, 0.39, 0.15, 0.21, 0.21, 0.25, 0.23, 0.50, 0.80
A (g)	1836, 1756, 1597, 1763, 1726, 1750, 1752, 1814, 1651, 1443
σ_A (g)	5, 59, 153, 88, 123, 109, 95, 41, 166, 221
I ($g*s/g_{peak}$)	0.0515, 0.0530, 0.0570, 0.0524, 0.0533, 0.0527, 0.0521, 0.0515, 0.0558, 0.0625
σ_I ($g*s/g_{peak}$)	0.0007, 0.0019, 0.0052, 0.0022, 0.0023 0.0020, 0.0018, 0.0006, 0.0063, 0.0089
F(1-25 Hz)	2.03, 2.04, 2.10, 2.05, 2.05, 2.04, 2.04, 2.04
F(26-50 Hz)	0.409, 0.443, 0.497, 0.433, 0.453, 0.439, 0.433, 0.412
F(51-75 Hz)	0.304, 0.323, 0.358, 0.320, 0.324, 0.313, 0.301, 0.302
F(76-100 Hz)	0.226, 0.240, 0.243, 0.234, 0.227, 0.223, 0.206, 0.213
F(101-200 Hz)	0.182, 0.177, 0.172, 0.171, 0.180, 0.179, 0.177, 0.179
F(201-300 Hz)	0.107, 0.102, 0.0970, 0.101, 0.111, 0.108, 0.112, 0.110
F(301-400 Hz) $*10^{-4}$	615, 568, 527, 588, 625, 605, 632, 632, 585, 608
F(401-600 Hz) $*10^{-4}$	226, 202, 165, 170, 184, 196, 213, 200, 165, 137
F(601-1000 Hz) $*10^{-4}$	29, 22, 16, 21, 17, 21, 25, 22, 18, 9
F(1001-1500 Hz) $*10^{-4}$	3.38, 1.26, 0.72, 1.06, 1.25, 1.65, 2.20, 1.63, 0.83, 0.72
F(1501-2000 Hz) $*10^{-4}$	0.41, 0.31, 0.30, 0.36, 0.26, 0.39, 0.38, 0.33, 0.46, 0.27
F(2001-3000 Hz) $*10^{-4}$	0.20, 0.17, 0.15, 0.16, 0.14, 0.19, 0.16, 0.19, 0.22, 0.17
F_{peak}	524, 526, 540, 535, 531, 524, 529, 537, 529, 540

Table E4: TMA-1 AT mine object features

Feature	Values
t_{wid} (ms)	1.82, 2.08, 2.00, 2.18, 2.00, 2.30, 2.67, 2.72
σ_{twid} (ms)	0.18, 0.12, 0.14, 0.35, 0.26, 0.33, 0.67, 0.45
A (g)	1838, 1836, 1836, 1801, 1790, 1752, 1634, 1581
σ_A (g)	0, 7, 4, 60, 149, 111, 279, 115
I ($g*s/g_{peak}$)	0.0509, 0.0515, 0.0515, 0.0515, 0.0518, 0.0527, 0.0573, 0.0570
σ_I ($g*s/g_{peak}$)	0.0009, 0.0006, 0.0006, 0.0012, 0.0027, 0.0029, 0.0104, 0.0046
F(1-25 Hz)	2.04, 2.05, 2.04, 2.05, 2.06, 2.04, 2.07 2.10
F(26-50 Hz)	0.389, 0.419, 0.405, 0.412, 0.395, 0.443, 0.493, 0.503
F(51-75 Hz)	0.302, 0.327, 0.307, 0.302, 0.314, 0.328, 0.345, 0.348
F(76-100 Hz)	0.212, 0.209, 0.219, 0.201, 0.196, 0.208, 0.220, 0.214
F(101-200 Hz)	0.185, 0.176, 0.178, 0.166, 0.168, 0.161, 0.164, 0.160
F(201-300 Hz)	0.125, 0.117, 0.118, 0.109, 0.113, 0.109, 0.105, 0.107
F(301-400 Hz) $*10^4$	875, 750, 777, 686, 791, 672, 689, 632
F(401-600 Hz) $*10^4$	285, 242, 271, 238, 234, 207, 193, 188
F(601-1000 Hz) $*10^4$	14.1, 11.2, 12.0, 14.8, 15.1, 11.2, 10.2, 11.8
F(1001-1500 Hz) $*10^4$	3.48, 0.97, 1.94, 1.13, 1.36, 0.51, 0.78, 0.71
F(1501-2000 Hz) $*10^4$	0.561, 0.291, 0.245, 0.246, 0.476, 0.258, 0.395, 0.322
F(2001-3000 Hz) $*10^4$	0.165, 0.159, 0.128, 0.119, 0.250, 0.188, 0.217, 0.195
F_{peak}	533, 528, 535, 539, 546, 524, 533, 540

Table E5: TMA-5A AT mine object features

Feature	Values
t_{wid} (ms)	4.72, 5.37, 5.40, 6.17, 6.15, 6.52, 2.40, 2.83
σ_{twid} (ms)	0.33, 1.32, 0.66, 1.32, 0.73, 1.03, 0.28, 0.41
A (g)	1105, 994, 923, 849, 813, 752, 1445, 1382
σ_A (g)	78, 116, 101, 117, 58, 89, 300, 195
I (g^*s/g_{peak})	0.108, 0.126, 0.135, 0.158, 0.158, 0.181, 0.066, 0.069
σ_I (g^*s/g_{peak})	0.010, 0.029, 0.022, 0.053, 0.016, 0.035, 0.015, 0.013
F(1-25 Hz)	2.78, 2.92, 3.01, 3.12, 3.09, 3.33, 2.19, 2.23
F(26-50 Hz)	1.23, 1.34E, 1.42, 1.47, 1.57, 1.72, 0.524, 0.564
F(51-75 Hz)	0.993, 0.997, 1.12, 1.17, 1.34, 1.37, 0.409, 0.436
F(76-100 Hz)	0.676, 0.676, 0.710, 0.710, 0.747, 0.740, 0.279, 0.301
F(101-200 Hz)	0.345, 0.348, 0.348, 0.327, 0.315, 0.299, 0.229, 0.242
F(201-300 Hz) $*10^4$	635, 551, 544, 453, 422, 389, 1267, 1048
F(301-400 Hz) $*10^4$	23, 35, 28, 40, 24, 39, 551, 416
F(401-600 Hz) $*10^4$	18, 13, 16, 13, 8, 16, 64, 53
F(601-1000 Hz) $*10^4$	6.45, 4.83, 8.25, 8.68, 3.45, 6.39, 4.33, 6.96
F(1001-1500 Hz) $*10^4$	1.19, 1.45, 1.84, 2.16, 0.85, 1.15, 1.52, 0.90
F(1501-2000 Hz) $*10^4$	0.639, 0.487, 0.318, 1.399, 0.696, 0.872, 0.362, 0.372
F(2001-3000 Hz) $*10^4$	0.195, 0.287, 0.138, 0.321, 0.255, 0.402, 0.198, 0.188
F_{peak}	594, 601, 621, 603, 614, 660, 579, 583

Table E6: TMA-4 AT mine object features

Feature	Values
t_{wid} (ms)	1.33, 1.67, 1.57, 0.95, 0.97, 0.95, 0.90, 1.20, 2.50, 1.45
σ_{twid} (ms)	0.14, 0.22, 0.23, 0.11, 0.15, 0.11, 0.09, 0.76, 0.33, 0.16
A (g)	1369, 1259, 1305, 1553, 1430, 1585, 1636, 1403, 618, 1305
σ_A (g)	35,116, 81, 248, 186, 104, 163, 298, 56, 87
I (g^*s/g_{peak})	0.0417, 0.0453, 0.0441, 0.0398, 0.0404, 0.0389, 0.0383, 0.0463, 0.1026, 0.0441
σ_I (g^*s/g_{peak})	0.0009, 0.0028, 0.0020, 0.0035, 0.0024, 0.0014, 0.0014, 0.0199, 0.0130, 0.0021
F(1-25 Hz)	1.94, 1.98, 1.98, 1.95, 1.96, 1.94, 1.92, 1.99, 2.38, 1.97
F(26-50 Hz)	0.165, 0.189, 0.187, 0.150, 0.153, 0.141, 0.140, 0.180, 0.517, 0.185
F(51-75 Hz) $*10^4$	966, 1115, 1064, 831, 868, 787, 757, 1044, 3582, 1091
F(76-100 Hz) $*10^4$	531, 656, 585, 422, 416, 416, 402, 585, 2419, 635
F(101-200 Hz) $*10^4$	554, 659, 622, 463, 429, 456, 429, 527, 2024, 662
F(201-300 Hz) $*10^4$	378, 405, 368, 355, 362, 362, 329, 375, 977, 395
F(301-400 Hz) $*10^4$	281, 300, 305, 351, 336, 335, 309, 333, 453, 325
F(401-600 Hz) $*10^4$	154, 166, 161, 229, 221, 219, 210, 212, 115, 179
F(601-1000 Hz) $*10^4$	82, 74, 75, 104, 97, 101, 102, 91, 10, 80
F(1001-1500 Hz) $*10^4$	22.6, 20.0, 20.5, 21.8, 23.3, 24.0, 25.5, 18.2, 1.4, 20.1
F(1501-2000 Hz) $*10^4$	6.35, 6.12, 6.18, 3.10, 3.99, 4.22, 4.46, 2.48, 0.74, 4.73
F(2001-3000 Hz) $*10^4$	0.591, 0.419, 0.527, 0.257, 0.463, 0.228, 0.358, 0.345, 0.378, 0.331
F_{peak}	586, 614, 621, 605, 608, 599, 585, 629, 732, 608

Table E7: Wood object features

Feature	Values
t_{wid} (ms)	2.12, 1.88, 1.78, 1.92, 1.90, 2.02, 1.87, 2.32, 2.07, 3.18, 2.50
σ_{twid} (ms)	0.08, 0.16, 0.16, 0.16, 0.18, 0.12, 0.11, 0.20, 0.58, 0.20, 0.52
A (g)	1717, 1676, 1748, 1724, 1746, 1800, 1765, 1408, 1638, 1191, 1478
σ_A (g)	200, 246, 155, 154, 155, 124, 174, 148, 166, 81, 222
I (g^*s/g_{peak})	0.0551, 0.0539, 0.0512, 0.0527, 0.0518, 0.0515, 0.0515, 0.0625, 0.0536, 0.0790, 0.0607
σ_I (g^*s/g_{peak})	0.0059, 0.0067, 0.0044, 0.0043, 0.0056, 0.0033, 0.0046, 0.0062, 0.0087, 0.0052, 0.0101
F(1-25 Hz)	2.01, 2.00, 1.98, 1.99, 1.99, 1.99, 1.98, 2.06, 1.96, 2.17, 2.01
F(26-50 Hz)	0.429, 0.392, 0.375, 0.395, 0.402, 0.385, 0.385, 0.527, 0.405, 0.723, 0.483
F(51-75 Hz)	0.321, 0.292, 0.265, 0.284, 0.281, 0.281, 0.278, 0.385, 0.285, 0.554, 0.358
F(76-100 Hz)	0.228, 0.208, 0.180, 0.202, 0.195, 0.201, 0.195, 0.267, 0.198, 0.392, 0.255
F(101-200 Hz)	0.199, 0.185, 0.166, 0.186, 0.169, 0.180, 0.172, 0.211, 0.158, 0.278, 0.187
F(201-300 Hz)	0.125, 0.116, 0.108, 0.122, 0.112, 0.116, 0.118, 0.136, 0.00980, 0.117, 0.109
F(301-400 Hz) $*10^4$	618, 666, 686, 723, 672, 689, 693, 706, 585, 382, 578
F(401-600 Hz) $*10^4$	126, 178, 209, 197, 204, 203, 218, 146, 158, 43, 141
F(601-1000 Hz) $*10^4$	6.15, 10.0, 13.8, 9.33, 13.9, 13.4, 13.7, 7.54, 15.6, 2.18, 11.6
F(1001-1500 Hz) $*10^4$	0.500, 0.733, 0.395, 0.419, 0.524, 0.564, 0.547, 4.83, 1.72, 0.490, 3.14
F(1501-2000 Hz) $*10^4$	0.249, 0.275, 0.223, 0.202, 0.243, 0.276, 0.289, 0.433, 0.355, 0.245, 0.426
F(2001-3000 Hz) $*10^4$	0.15, 0.15, 0.15, 0.15, 0.17, 0.16, 0.15, 0.28, 0.15, 0.15, 0.17
F_{peak}	500, 498, 511, 513, 491, 502, 506, 489, 533, 443, 539

Table E8: Steel object features

Feature	Values
t_{wid} (ms)	0.567, 0.650, 0.583, 0.633, 0.683, 0.800, 0.700
σ_{twid} (ms)	0.086, 0.095, 0.088, 0.070, 0.095, 0.312, 0.105
A (g)	1825, 1827, 1792, 1772, 1770, 1472, 1623
σ_A (g)	40, 34, 106, 111, 85, 386, 152
I (g^*s/g_{peak})	0.0352, 0.0355, 0.0349, 0.0355, 0.0355, 0.0407, 0.0365
σ_I (g^*s/g_{peak})	0.0005, 0.0004, 0.0005, 0.0007, 0.0006, 0.0133, 0.0009
F(1-25 Hz)	1.92, 1.89, 1.89, 1.91, 1.91, 1.96, 1.91
F(26-50 Hz)	0.110, 0.109, 0.104, 0.111, 0.111, 0.132, 0.117
F(51-75 Hz)	554, 551, 527, 568, 578, 747, 622
F(76-100 Hz)	243, 246, 230, 258, 269, 348, 288
F(101-200 Hz)	266, 260, 238, 267, 269, 319, 287
F(201-300 Hz)	226, 226, 192, 216, 224, 245, 240
F(301-400 Hz) $*10^4$	230, 233, 204, 223, 227, 243, 242
F(401-600 Hz) $*10^4$	174, 173, 155, 167, 166, 157, 176
F(601-1000 Hz) $*10^4$	113, 108, 103, 105, 103, 89, 106
F(1001-1500 Hz) $*10^4$	47.0, 40.5, 41.0, 36.8, 36.5, 35.5, 35.5
F(1501-2000 Hz) $*10^4$	12.4, 9.7, 12.7, 10.4, 10.3, 9.7, 8.7
F(2001-3000 Hz) $*10^4$	1.34, 1.03, 1.69, 1.23, 1.33, 1.28, 0.98
F_{peak}	597, 568, 572, 586, 588, 616, 575